



(11) **EP 2 243 425 B1**

(12) **EUROPEAN PATENT SPECIFICATION**

(45) Date of publication and mention of the grant of the patent:  
**13.08.2014 Bulletin 2014/33**

(51) Int Cl.:  
**A61B 5/1455** <sup>(2006.01)</sup> **A61B 5/00** <sup>(2006.01)</sup>

(21) Application number: **10170622.4**

(22) Date of filing: **30.11.2006**

(54) **Method for noninvasive measurement of glucose and apparatus for noninvasive measurement of glucose**

Verfahren zur nicht invasiven Messung von Glukose und Vorrichtung zur nicht invasiven Messung von Glukose

Procédé de mesure non-invasive de glucose et appareil pour mesure non-invasive de glucose

(84) Designated Contracting States:  
**DE**

(30) Priority: **30.11.2005 JP 2005347194**  
**08.05.2006 JP 2006129490**

(43) Date of publication of application:  
**27.10.2010 Bulletin 2010/43**

(60) Divisional application:  
**11180748.3 / 2 399 515**  
**11180771.5 / 2 399 516**  
**11180786.3 / 2 399 517**

(62) Document number(s) of the earlier application(s) in accordance with Art. 76 EPC:  
**06833798.9 / 1 955 653**

(73) Proprietor: **Toshiba Medical Systems Corporation**  
**Otawara-shi,**  
**Tochigi-ken 324-8550 (JP)**

(72) Inventors:

- **Kanayama, Shoichi**  
**Tochigi-ken 324-8550 (JP)**
- **Khalil, Omar, S.**  
**Tochigi-ken 324-8550 (JP)**
- **Jeng, Tzyy-Wen**  
**Tochigi-ken 324-8550 (JP)**
- **Yeh, Shu-Jen**  
**Abbott Park, IL 60064-3500 (US)**

(74) Representative: **Kramer - Barske - Schmidtchen**  
**Landsberger Strasse 300**  
**80687 München (DE)**

(56) References cited:  
**WO-A-01/87151 WO-A-02/060320**  
**WO-A1-02/082989 US-B2- 6 954 661**

**EP 2 243 425 B1**

Note: Within nine months of the publication of the mention of the grant of the European patent in the European Patent Bulletin, any person may give notice to the European Patent Office of opposition to that patent, in accordance with the Implementing Regulations. Notice of opposition shall not be deemed to have been filed until the opposition fee has been paid. (Art. 99(1) European Patent Convention).

**Description**

## Technical Field

5 **[0001]** The present invention relates to an apparatus and a method for noninvasive measurement, with which glucose in a subject is noninvasively measured optically through a measurement probe.

## Background Art

10 **[0002]** In several prior art methods, noninvasive (NI) measurement of glucose concentration in a subject is described. This measurement method generally includes the steps of: bringing an optical probe into contact with a body part; performing a series of optical measurements; and collecting a series of light signals. Subsequently, these light signals or derived optical parameters are mutually associated with blood glucose concentrations for the establishing a calibration relationship. A glucose concentration is determined by a subsequent measurement using the light signals measured at  
15 that time and the previously established calibration relationship.

**[0003]** The method for noninvasive (NI) measurement of glucose is classified into two broad categories: one is a method of tracking molecular properties; and the other is a method of tracking the effect of glucose on tissue properties. The method in the first category includes tracking intrinsic properties of glucose such as near-infrared (NIR) absorption coefficients, mid-infrared absorption coefficients, optical rotations, Raman shift band and NIR photoacoustic absorption.  
20 Such a method is based on an ability to detect glucose in a tissue or blood independently of other analytes of the body and also physiological conditions of the body. The method of the second type is based on the measurement of the effect of glucose on optical properties of tissue such as scattering coefficients of tissue, refractive index of interstitial fluid (ISF) or sound propagation in tissue.

**[0004]** The method of the first type of tracking the molecular properties of glucose faces a big problem because a  
25 signal which can be considered to be specific for glucose is extremely weak. Biological noise, a person-to-person difference, and measurement noise may drown out a small change in signal specific for glucose. In order to extract glucose-related information from a data set with noise, a multivariate analysis has been commonly used. The method of the second type of tracking the effect of glucose on tissue properties instead of the intrinsic molecular properties of glucose faces a big problem because of a nonspecific property of the change in parameters to be measured.

30 **[0005]** The method of both types of tracking the molecular properties of glucose and the effect of glucose on tissue properties ignores the physiological response of the body to a change in glucose concentration. This response can be seen in the form of a change in blood flow or temperature. Such a change in blood flow or temperature as a result of the physiological response of the body affects NIR light signals. The measurement by the method of both types also ignores the effect of the body-probe interaction on signals measured, and further, a specific time window for data collection  
35 from the initiation of the body-probe interaction is not defined.

## Absorption method:

40 **[0006]** Patent documents 1, 2, 3, 4, 5, 6, 7 and 8 describe a method in which glucose is measured by bringing an optical probe into contact with a body part and also reflection or transmission signals in near-infrared (NIR) region ranging from 600 to 1100 nm are measured. In general, a blood-containing body part (such as a finger) is illuminated with one or more light wavelengths, and one or more detectors detect the light passing through the body part. A glucose level is derived from the comparison of the reference spectrum of glucose and the background interference. These patents do not deal with the physiological response of the body to a change in glucose concentration, or the tissue-probe adaptation effect on the light signals measured.  
45

**[0007]** In patent documents 9, 10 and 11, measurement of glucose NIR signals at a long wavelength ranging from 1000 to 1800 nm has been claimed. These patents disclose a method in which an extremely low signal is tried to be measured in the presence of biological noise which is much larger than the signal. The method of these patents does not provide temperature modulation at the measurement site, and these patents do not deal with the physiological response to a change in glucose concentration or the response of the body to the probe when the body and the probe interact with each other during the measurement.  
50

**[0008]** Patent documents 12 to 19 disclose a method for NI measurement of glucose using NIR reflectance and transmittance measurement at a wavelength ranging from 1000 to 2000 nm. These patents do not deal with the physiological response of the body to glucose or problems of the probe-tissue interaction, or describe the application of temperature stimulation.  
55

**[0009]** An example of the magnitude of NIR glucose intrinsic absorption signals is illustrated by the recently measured values of the molar extinction coefficient  $\epsilon$  of glucose in water reported in the article in the journal (Non-patent document 1). The absorption ratio of glucose in water was determined to be  $0.463 \text{ M}^{-1}\text{cm}^{-1}$  at 1689 nm,  $0.129 \text{ M}^{-1}\text{cm}^{-1}$  at 2270 nm

and  $0.113 \text{ M}^{-1}\text{cm}^{-1}$  at 2293 nm (here, M represents a molar concentration). These values of absorption ratios are much smaller than the  $\epsilon$  value of NADH at 340 nm being  $6.2 \times 10^{+3} \text{ mol}^{-1}\text{cm}^{-1}$ , which is commonly used for the measurement of serum glucose values with an automated blood analyzer. When a 1 mm pathlength is used, a 10 mM glucose solution has  $4.63 \times 10^{-4}$  absorbance units at 1686 nm, and  $1.29 \times 10^{-4}$  absorbance units at 2257 nm. The 1 mm pathlength is longer than the pathlength encountered in the NIR diffuse reflectance measurement, and has a magnitude comparable to the pathlength in the localized reflectance measurement. The intrinsic extinction coefficient of glucose has a magnitude much lower at the higher overtone bands between 800 nm and 1300 nm than that at 2200 nm. The quantitative interpretation of data in this spectral range requires an extremely high sensitive detection system with a high signal to noise ratio and tight temperature modulation, and elimination of biological background noise source. Although IR absorption measurement of glucose has reasonable specificity in aqueous solutions, it faces a serious problem when attempted at the body sites of a subject.

**[0010]** The earliest report of use of measurement of NIR absorption and reflectance was reported in 1992 (Non-patent document 2), however, a commercially available device for noninvasive measurement of glucose by NIR has been unavailable so far.

Scattering method:

**[0011]** Patent document 20 by Simonsen et al. and Patent document 21 by Gratton et al. disclose a method of measuring a scattering coefficient in deep tissue structures such as calf muscle and abdominal area. The geometric arrangement of a measurement probe, a distance between a light source and a detecting point, and the use of diffusion approximation in a light transport equation require light sampling at a depth of about several centimeters in a tissue.

**[0012]** A scattering method for NI measurement of glucose is described in the articles in the literatures of Non-patent documents 3, 4, and 5. In the method using the effect of glucose on the magnitude of a tissue scattering coefficient, a change in refractive index of interstitial fluid (ISF) which is resulted from a change in glucose concentration is tracked. The effect of a solute concentration on the refractive index of a solution is not specific for a given compound. A change in other soluble metabolite and electrolyte concentrations or tissue hydration affects the refractive index in the same manner as a change in glucose concentration. The reported clinical results have showed that there is no specificity and it is impossible to predict a glucose concentration

(Non-patent document 6).

**[0013]** The effect of changing temperature on tissue scattering and absorption properties has been very interesting in noninvasive monitoring techniques. This has been reported in a few articles in journals. Please see Non-patent documents 7 and 8. The effect of temperature on the optical properties of the human skin has been reported in the articles in the journals of Non-patent documents 9, 10, 11 and 12. These published reports show a reversible linear change in scattering coefficient of the human skin after changing the temperature, and a more irreversible change in skin absorption coefficient after changing the temperature. Thermal radiation method:

**[0014]** Other patents and patent application publications disclose a method which depends on IR radiation from a subject. In Patent documents 22 and 23 by Sterling et al., altered thermal IR radiation was used for NI measurement of glucose. The use of metabolic thermal radiation from a subject as means for glucose measurement has been disclosed in Patent documents 24 and 25 by Cho et al., and Patent document 26 (June, 2005) and Patent document 27 (June, 2005). A few experimental data have been disclosed in the articles in the journals: Non-patent documents 13 and 14. Cho et al. did not separate the circadian effect of the body which causes a temperature change from a change in glucose concentration which may cause a temperature change in a similar manner. Cho et al. did not take the skin-probe adaptation effect on the optical or thermal signals into consideration, or did not generate a temperature change that affects glucose metabolism.

**[0015]** Patent document 28 by Buchert and the article of the journal of Non-patent document 15 describe a method for NI measurement of glucose based on a spectral analysis of IR radiation from the tympanic membrane. Buchert and Malchoff et al. did not induce a temperature change for affecting glucose metabolism.

**[0016]** The use of a temperature change in combination with optical measurement with respect to a subject is described in other NI optical measurements. Patent documents 29, 30, 31, 32, 33 and 34 describe an oximeter probe having a heating element designed such that it is disposed against a body part. In Patent document 35, a glucose sensor which is brought to a specified temperature and in which a scattering coefficient  $\mu_s'$  is calculated is described and a glucose concentration is estimated from the effect on the refractive index of interstitial fluid (ISF). Patent document 35 does not disclose the calculation of oxygen consumption as a result of the physiological effect of glucose metabolism, or describe the use of temperature-enhanced glucose metabolism, or disclose the use of time window for reducing the tissue-probe adaptation effect on the measurement to the minimum.

**[0017]** Patent document 36 by Mills describes a method for measuring blood parameters at various temperatures

based on the measurement of diffuse reflectance or transmission. Patent document 36 does not disclose the calculation of oxygen consumption as a result of the physiological effect of glucose metabolism, or describe the use of temperature-enhanced glucose metabolism, or take the time window for reducing the tissue-probe adaptation effect on the measurement to the minimum into consideration.

5 [0018] Although there are a variety of prior art and a large number of published patents in the past 10 years, however, any of the methods of noninvasive detection of glucose in a human tissue was not commercially successful. Accordingly, a method for noninvasive measurement of glucose in a subject which overcomes the problems of the signal magnitude and specificity, and without resorting to insertion of a probe or extraction of a sample has been still needed.

10 [0019] Further, several prior art methods for noninvasive (NI) quantification of the concentration of an analyte, particularly glucose in a subject generally includes the steps of: bringing a measurement probe into contact with a body part; performing a series of optical measurements; and collecting a set of light signals. These light signals or derived optical parameters calculated from the signals are mutually associated with blood glucose concentrations for establishing a calibration relationship. A glucose concentration is determined by a subsequent measurement using the light signals measured at that time and the previously established calibration relationship.

15 [0020] The method for noninvasive (NI) determination of glucose is classified into two broad categories: one is a method of tracking molecular properties; and the other is a method of tracking the effect of glucose on tissue properties. The method in the first category includes tracking intrinsic properties of glucose such as near-infrared (NIR) absorption coefficients, mid-infrared absorption coefficients, optical rotations, Raman shift band and NIR photoacoustic absorption. Such a method is based on an ability to detect glucose in a tissue or blood independently of other analytes of the body and also physiological conditions of the body. The method of the second type depend on the measurement of the effect of glucose on optical properties of tissue such as scattering coefficients of tissue, refractive index of interstitial fluid (ISF) or sound propagation in tissue.

20 [0021] The method of the first type of tracking the molecular properties of glucose encounters an extremely weak signal which can be considered to be specific for glucose. Biological noise, a person-to-person variation, and measurement noise may drown out a small change in the signal specific for glucose. In order to extract glucose-related information from a data set with noise, a multivariate analysis has been commonly used. The method of the second type of tracking the effect of glucose on tissue properties faces a big problem because of a nonspecific property of the change in refractive index calculated from the change in scattering coefficient.

25 [0022] In either type of methods, the intensity of the detected signal is extremely smaller than that of the biological and bodily interface noise. The variable probe-skin interaction which is attributable to the variation in the interface between a probe and the body, and a variable contact between a measurement probe and the skin due to the error of repositioning of the probe can have an effect on a measured signal which is larger than an effect on a change in glucose concentration.

30 [0023] The prior art method of both types of tracking the molecular properties of glucose and the effect of glucose on tissue properties ignores the effect of the body-probe interaction on the measured signal, and a method for reducing this effect is not described. As a result, a reference value of glucose is generally applied (fitted) to a signal adversely affected by an optical effect of an interaction between a probe and the skin or a probe and a body part.

35 [0024] Patent documents 37 to 44 describe a light absorption method for measuring reflection or transmission signals in near-infrared (NIR) region ranging from 600 to 1100 nm for measuring glucose by bringing a measurement probe into contact with a body part. In general, a blood-containing body part (such as a finger or a skin region of an arm) is illuminated with one or more wavelength lights, and one or more detectors detect the light passing through the body part or reflecting from the body part. A glucose level is derived from the comparison of the reference spectrum of glucose and the background interference. These patent documents do not deal with the tissue-probe adaptation effect on the light signals measured.

40 [0025] In Patent documents 45, 46 and 47, measurement of glucose NIR signals at a long wavelength ranging from 1000 to 1800 nm has been claimed. The method of these patent documents does not deal with a reaction of the skin with a measurement probe when the measurement probe interacts with the skin during measurement.

45 [0026] Patent documents 48, 49 and 50 transferred to Sensys Medical, Patent documents 51 and 52 transferred to Matsushita, and Patent documents 53, 54 and 55 transferred to Inlight Solutions disclose a method for NI quantification of glucose using measurement of NIR reflectance and transmission at a wavelength ranging from 1000 to 2000 nm. These patent documents do not deal with problems of the probe-tissue interaction, particularly adaptation of the skin to a probe and a variability of contact between the skin and a measurement probe.

50 [0027] Patent document 56 by Simonsen et al. and Patent document 57 by Gratton et al. disclose a method for measuring a bulk scattering coefficient in deep tissue structures such as calf muscle and abdominal area. The published clinical results show that it lacks specificity and glucose concentration cannot be predicted (Non-patent document 16). A drift (change) in the signal independent of glucose was observed, and it was larger than a change in scattering coefficient due to a change in glucose concentration in some cases.

55 [0028] In Patent document 56, a glucose sensor that is brought to a specified temperature is described and a bulk scattering coefficient is calculated, and a glucose concentration is estimated from the effect on the refractive index of

interstitial fluid (ISF). Patent document 56 does not disclose a method for reducing the effect of tissue-probe adaptation on the measurement to the minimum.

**[0029]** Patent document 58 by Mills describes a method for measuring blood parameters at various temperatures based on the measurement of diffuse reflectance or transmission. Patent document 58 does not disclose a method for reducing the effect of tissue-probe adaptation on the measurement to the minimum.

5

10

15

20

25

30

35

40

45

50

55

- Patent document 1: US Patent No. 5077476
- Patent document 2: US Patent No. 5068536
- Patent document 3: US Patent No. 5576544
- Patent document 4: US Patent No. 5703364
- Patent document 5: US Patent No. 5028787
- Patent document 6: US Patent No. 5086229
- Patent document 7: US Patent No. 5324979
- Patent document 8: US Patent No. 5237178
- Patent document 9: US Patent No. 5360004
- Patent document 10: US Patent No. 5460177
- Patent document 11: US Patent No. 5379764
- Patent document 12: US Patent No. 5747806
- Patent document 13: US Patent No. 5945676
- Patent document 14: US Patent No. 6280381
- Patent document 15: US Patent No. 5957841
- Patent document 16: US Patent No. 6016435
- Patent document 17: US Patent No. 5636633
- Patent document 18: US Patent No. 5655530
- Patent document 19: US Patent No. 6230034
- Patent document 20: US Patent No. 5551422
- Patent document 21: US Patent No. 5492118
- Patent document 22: US Patent No. 6049081
- Patent document 23: US Patent No. 6556850
- Patent document 24: US Patent No. 5795305
- Patent document 25: US Patent No. 5924996
- Patent document 26: US Patent Application Publication No. 2005/0124868
- Patent document 27: European Patent Application Publication No. 1537822
- Patent document 28: US Patent No. 5940182
- Patent document 29: US Patent No. 3628525
- Patent document 30: US Patent No. 4259963
- Patent document 31: US Patent No. 4432365
- Patent document 32: US Patent No. 4890619
- Patent document 33: US Patent No. 4926867
- Patent document 34: US Patent No. 5131391
- Patent document 35: US Patent No. 5551422
- Patent document 36: US Patent No. 5978691
- Patent document 37: US Patent No. 5,077,476
- Patent document 38: US Patent No. 5,068,536
- Patent document 39: US Patent No. 5,576,544
- Patent document 40: US Patent No. 5,703,364
- Patent document 41: US Patent No. 5,028,787
- Patent document 42: US Patent No. 5,086,229
- Patent document 43: US Patent No. 5,324,979
- Patent document 44: US Patent No. 5,237,178
- Patent document 45: US Patent No. 5,360,004
- Patent document 46: US Patent No. 5,460,177
- Patent document 47: US Patent No. 5,379,764
- Patent document 48: US Patent No. 5,747,806
- Patent document 49: US Patent No. 5,945,676
- Patent document 50: US Patent No. 6,280,381
- Patent document 51: US Patent No. 5,957,841
- Patent document 52: US Patent No. 6,016,435

Patent document 53: US Patent No. 5,636,633

Patent document 54: US Patent No. 5,655,530

Patent document 55: US Patent No. 6,230,034

Patent document 56: US Patent No. 5,551,422

5 Patent document 57: US Patent No. 5,492,118

Patent document 58: US Patent No. 5,978,691

Non-Patent document 1: Amerov et al., "Molar absorptivities of glucose and other biological molecules in aqueous solutions over the first overtone and combination regions of the near-infrared spectrum", *Applied Spectroscopy* 58: 1195-1204 (2004)

10 Non-Patent document 2: Robinson et al., "Noninvasive glucose monitoring in diabetic patients: a preliminary evaluation", *Clinical Chemistry* 1992 Sep; 38(9): 1618-22

Non-Patent document 3: Maier et al., "Non-invasive glucose determination by measuring variations of the reduced scattering coefficient of tissues in the near-infrared", *Optics Letter* 1994; 19: 2062-64

15 Non-Patent document 4: Kohl et al., "Influence of glucose concentration on light scattering in tissue stimulating phantoms", *Optics Letters* 1994; 19: 2170-72 Non-Patent document 5: Kohl et al., "The influence of glucose concentration upon the transport of light in tissue-stimulating phantoms", *Physics Medicine Biology* 1995; 40: 1267-87

Non-Patent document 6: Heinmann et al., *Diabetes Technology Therapeutics* 2000; 2: 211-220

Non-Patent document 7: Laufer et al., "Effect of temperature on the optical properties of ex vivo human dermis and subdermis", *Phys. Med. Biol.* (1998) volume 43: 2479-2489

20 Non-Patent document 8: Bruulsema et al., "Optical Properties of Phantoms and Tissue Measured in vivo from 0.9-1.3  $\mu\text{m}$  using Spatially Resolved Diffuse Reflectance", *SPIE Proceedings* 2979 (1997) 325-334 Non-Patent document 9: Khalil et al., "Temperature modulation of the visible and near infrared absorption and scattering coefficients of intact human skin", *J Biomedical Optics*, 2003; 8: 191-205

Non-Patent document 10: Yeh et al., "Near Infrared Thermo-Optical Response of The Localized Reflectance of Intact Diabetic and Non-Diabetic Human Skin", *J Biomedical Optics*, 2003; 8: 534-544

25 Non-Patent document 11: Yeh et al., "Tracking Blood Glucose Changes in Cutaneous Tissue by Temperature-Modulated Localized Reflectance Measurements", *Clinical Chemistry* 2003; 49: 924-934

Non-Patent document 12: Khalil et al., "Response of near IR localized reflectance signals of intact diabetic human skin to thermal stimuli", *SPIE Proceedings* 2003; 5086: 142-148

30 Non-Patent document 13: Cho et al., "Noninvasive measurement of glucose by metabolic heat conformation method", *Clinical Chemistry* 2004; 50: 1984-1988

Non-Patent document 14: Ko et al., "Body metabolism provides a foundation for noninvasive blood glucose monitoring", *Diabetes Care*, 2004; 27: 1211-2

35 Non-Patent document 15: Malchoff et al., "A novel noninvasive blood glucose monitor", *Diabetes Care* 2002; 25: 2268-75

Non-Patent document 16: Heinemann et al., *Diabetes Technology Therapeutics* 2000; 2: 211-220

[0030] WO 02/082989 A1 discloses a method for the determination of a disease state in a tissue of a human, said method comprising the steps of (a) measuring at least one optical property at a first area on said tissue to obtain a first set of data, said first area being subjected to a first temperature program, (b) measuring at least one optical property at a second area on said tissue to obtain a second set of data, said second area being subjected to a second temperature program, said second temperature program being different from the first temperature program, said second area being morphologically similar to but not substantially overlapping with said first area, (c) inserting said first set of data and said second set of data into a mathematical relationship to calculate a mathematical output, and (d) comparing said mathematical output to a category selector to determine said disease state of said human.

#### Disclosure of Invention

[0031] An object of the present invention is to track temperature-induced glycolysis by inducing a temperature change in the human skin, measuring localized reflectance signals at several defined light source-detector distances, and correlating functions derived from the reflectance values obtained at a plurality of wavelengths and light source-detector distances with glucose concentrations in a method for noninvasive measurement of glucose and an apparatus for noninvasive measurement of glucose.

#### Brief Description of Drawings

[0032]

FIG. 1 is a diagram showing a configuration of an apparatus for noninvasive measurement of glucose according to a first embodiment.

FIG. 2 is a diagram showing a structure of a read head of the apparatus for noninvasive measurement of FIG. 1.

FIG. 3 shows functions of oxygen consumption obtained by using a probe at 40°C with respect to various light source-detector distances. Lozenges indicate 0.559 mm, circles indicate 0.879 mm, triangles indicate 1.318 mm, and Xs indicate 1.758 mm.

FIG. 4 shows  $F(OC)$  obtained by using a probe at 40°C. The time window was between 0 and 90 sec. Data was normalized to 5 sec data point. Lozenges indicate 0.559 mm, circles indicate 0.879 mm, triangles indicate 1.318 mm, and Xs indicate 1.758 mm. The lines are linear least squares approximation lines.

FIG. 5 shows a plot of  $\ln(R_4/R_1)$  against time with respect to a probe heated to 40°C. Lozenges indicate 592 nm, circles indicate 660 nm, Xs indicate 880 nm, and triangles indicate 940 nm.

FIG. 6 shows simulation of profile of change in oxygen consumption rate when the skin is brought into contact with a probe heated such that the temperature thereof is increased by about 10°C.

FIG. 7A is a Clarke Error Grid diagram for noninvasive measurement of glucose using the equation 37. Lozenges indicate calibrated data points and circles indicate predicted glucose values. The line is an approximation line between predicted and actual glucose values.

FIG. 7B is a Clarke Error Grid diagram for noninvasive measurement of glucose using the equation 38. Lozenges indicate calibrated data points and circles indicate predicted glucose values. The line is an approximation line between predicted and actual glucose values.

FIG. 7C is a Clarke Error Grid diagram for noninvasive measurement of glucose using the equation 39. Lozenges indicate calibrated data points and circles indicate predicted glucose values. The line is an approximation line between predicted and actual glucose values.

FIG. 7D is a Clarke Error Grid diagram for noninvasive measurement of glucose using the equation 40. Lozenges indicate calibrated data points and circles indicate predicted glucose values. The line is an approximation line between predicted and actual glucose values.

#### Best Mode for Carrying Out the Invention

(First embodiment)

**[0033]** A first embodiment of the present invention relates to a method for noninvasive measurement of glucose concentration in a subject. The method utilizes a property that transient glucose metabolism is affected by temperature and a light signal changes according to a change in the metabolism.

**[0034]** In the first embodiment of the invention, a temperature-modulated localized reflectance optical probe which is similar to a probe described in US Patent No. 6662030 by Khalil et al. and Khalil et al., J. Biomed. Opt. 2003; 8: 191-205, Yeh et al., J. Biomed. Opt. 2003; 8: 534-44, and Yeh et al., Clin. Chem. 2003; 49: 924-34 is used. In the measurement of localized reflectance signals using a temperature-modulated probe described in US Patent No. 6662030 (Khalil et al.), a light signal is generated according to a contact time between the probe at a temperature or a given temperature and a body part. The detected signal corresponds to light absorption by tissue chromophores and red blood cells, and light scattering from the center of tissue scattering and red blood cells. The visible and NIR light absorption by the blood mainly attributes to the light absorption by a hemoglobin variant in red blood cells (RBC). The variant includes oxyhemoglobin (about 95%) and deoxyhemoglobin (about 5%).

**[0035]** When a solid substance such as an optical probe comes into contact with the skin, several mechanical effects are caused. The probe presses the skin to cause local occlusion and further affects blood flow. In a similar manner, heat is transferred from the probe to the skin or vice versa depending on the thermal conductivity of a material of the probe and a difference in the temperature between the tissue and the probe. The adaptation of the soft skin to the rigid metal probe can appear as a time dependent change in measured light signal. The heat transfer to the skin induces a temporary temperature change at a measurement site. A subsequent temperature change in a nutrient capillary in the skin is caused followed by widening of a blood vessel and opening of capillary shunts. Most of the capillary shunts begin to open at 42°C and completely open at 46°C.

**[0036]** Glucose is metabolized in human tissues in a continuous manner. A change in glucose metabolism has been used for detecting a tumor activity by injecting radioactive glucose into the vein of a patient and observing radioactive distribution in tissues by positron emission tomography (PET). Oxygen consumption in the brain has been calculated from NIR light signals for showing a cognitive activity. Oxygen consumption has been measured also in a tumor for detecting angiogenesis and excess metabolism in the tumor. Another method for measuring oxygen consumption is magnetic resonance of iron atoms in oxyhemoglobin and deoxyhemoglobin. This technique is called a functional magnetic resonance imaging method.

**[0037]** In glucose metabolism in a subject, there are three pathways, i.e., glycolysis, conversion into lipids, and glucose

storage as glycogen. Glycolysis is oxidation of glucose into CO<sub>2</sub> and water, and takes place in all the living cells. Glucose conversion into lipids takes place in adipose tissues and muscle and liver cells. Glucose storage as glycogen takes place in liver cells.

**[0038]** In the first embodiment, the effect of temperature on glucose metabolism in the blood, particularly in red blood cells is employed. Red blood cells (also known as erythrocytes) cannot store glucose or use other substrates as an energy. Glycolysis is a major metabolic pathway of glucose in red blood cells. An oxygen source in red blood cells is oxygen transport protein hemoglobin. Transport of glucose (G) to red blood cells is instantaneous. Glucose is metabolized into carbon dioxide and water in RBC or remains there as a free glucose molecule. The free glucose in red blood cells causes glycosylation of hemoglobin to form glycosylated hemoglobin, HbA1c, which is a marker of poor blood glucose regulation. An increase in glucose concentration to a level exceeding a normal nondiabetic range leads to an increase in HbA1c concentration. A high HbA1c level is a sign of the onset of frequent hyperglycemia.

**[0039]** In the first embodiment, a temperature jump effect on a glycolysis process is used. In glycolysis in red blood cells, physically dissolved oxygen (smaller portion) or oxygen transported by hemoglobin, which is an oxygen transport protein, is consumed. An oxyhemoglobin molecule dissociates into deoxyhemoglobin and oxygen. A change in glucose metabolism leads to an instantaneous change in HbO<sub>2</sub> concentration. Subsequently, oxidized hemoglobin is supplied at a measurement site by breathing and blood flow. In the first embodiment of the invention, these effects are tracked by measuring the effects of temperature stimulation on localized reflectance signals at a plurality of wavelengths corresponding to light absorption by an oxidized hemoglobin variant.

**[0040]** In the first embodiment, the effect of temperature on glucose metabolism with respect to light scattering from the blood and a tissue component is used. A scattering coefficient in a tissue is determined by the refractive index mismatch between the center of tissue scattering and ISF. The refractive index  $n_{ISF}$  of ISF is non-specific for glucose, but determined by a glucose concentration. US Patent Nos. 5551422 and 5492118 disclose the use of a scattering coefficient change for NI measurement of glucose. The subject experiment (Diabetes Technology and Therapeutics 2000; 2: 211-220) shows nonspecificity of the effect and lack of correlation with glucose. A change in glycolysis induces a change in refractive index as glucose molecules in the blood are consumed. By incorporating a change in scattering and absorption when changing the temperature, specificity of signals measured can be provided.

**[0041]** The first embodiment is a method for noninvasive measurement of glucose in a subject. The method includes bringing a localized reflectance optical probe whose temperature has been set to a temperature substantially different from the normal temperature of the human skin into contact with the skin for inducing a sudden temperature change in the skin tissue. A temperature-enhanced change in glucose metabolism (glycolysis) in red blood cells is caused, and oxygen is consumed. There is a temporary stoichiometric relationship between glucose and HbO<sub>2</sub> concentration. This relationship can be a source of signal specificity. The oxygen consumption in RBC can be calculated from light absorption by red blood cells at various wavelengths and various light source-detector distances.

**[0042]** According to the first embodiment, the localized reflectance probe whose temperature is substantially different from the normal temperature of a tissue is brought into contact with the human skin, whereby a change in glucose concentration associated with the ambient glucose concentration is induced. As a result of this perturbation, the glucose concentration can be expressed in terms of a physical parameter and a physiological parameter. The physical parameter is associated with a rate of change in effective attenuation coefficient according to the probe-skin contact time. Further, a change in blood flow, widening of a blood vessel and scattering by tissue and blood cells will be induced. The physiological parameter is associated with a rate of oxygen consumption according to the probe-skin contact time.

**[0043]** According to the first embodiment, a temperature higher than the normal temperature of the skin can cause enhanced glycolysis in a nutrient capillary before the capillary system reaches an equilibrium with ambient tissues by widening of a blood vessel.

**[0044]** According to the first embodiment, glycolysis in RBC is dependent on temperature. The rate of glycolysis changes as a temperature changes in a range from 30 to 42°C. The rate is constant at a body core temperature of 37°C. A skin temperature is lower than the body core temperature. A sudden increase in temperature in a short time of about 60 sec can cause a change in the consumption of oxygen in a capillary and a rate of glycolysis before oxygen is supplied by blood flow and normal breathing.

**[0045]** According to the first embodiment, a blood glucose concentration affects a rate of glycolysis in a nutrient capillary and the response to the thermal stimulation. The rate of glycolysis is determined by an initial glucose concentration in red blood cells and therefore by a blood glucose concentration. The degree of glycolysis over a defined time from the initiation of temperature-induced glycolysis is determined by an initial glucose concentration in red blood cells and therefore by a blood glucose concentration. When quasi-one dimensional rate is used, the rate of glycolysis can be represented as follows.

$$d[G]/dt = -k_1[G]_{RBC} \quad (1)$$

$$[G]_{RBC} = \chi [G]_{Blood} \quad (2)$$

( $\chi$  represents a partition coefficient which is a fractional number determined by the diabetic conditions, insulin concentration and insulin sensitivity of a human.)

**[0046]** In another aspect of the first embodiment, a rate of change in glycolysis is associated with a rate of oxygen consumption in red blood cells, and can be measured at at least two wavelengths, and the at least two wavelengths have values substantially different with respect to the extinction coefficient of deoxyhemoglobin and that of oxyhemoglobin. Oxygen consumption in RBC is calculated according to a time from the initiation of contact of the skin with the measurement probe having a temperature substantially different from an ambient skin temperature.

$$d[G]/dt \approx -k_2 d[HbO_2]/dt = k_3 d[\text{oxygen consumption}]/dt \quad (3)$$

and

$$d[G]/dt \approx k_4 d\mu_{eff}/dt \quad (4)$$

**[0047]** A glucose concentration can be represented as follows based on the assumption of one-dimensional kinetics.

$$[G] \approx k_4 d[\text{oxygen consumption}]/dt \quad (5)$$

and

$$[G] \approx k_5 d\mu_{eff}/dt \quad (6)$$

**[0048]** According to the first embodiment, a glucose concentration can be calculated from the sum of two responses as follows.

$$[G] = \sum_i [f_{1i}(\text{physical response})] + \sum_j [f_{2j}(\text{physiological response})] \quad (7)$$

**[0049]** In another aspect of the first embodiment, a change in relative reflectance at two wavelengths corresponding to light absorption by a hemoglobin variant is caused as a result of thermal stimulation applied to a nutrient capillary. This change in absorption by hemoglobin in the capillary bed is used as an index of the degree of glucose metabolism or the rate of glycolysis in red blood cells. Glycolysis is the only metabolic pathway of glucose in red blood cells, therefore, a change in oxidized state of hemoglobin is an index specific for glycolysis and can be used as an index of a blood glucose concentration. The rate of oxygen consumption and the degree of oxygen consumption can be used as a physiological parameter and also can have a correlation with a change in glucose concentration.

**[0050]** US Patent No. 6662030 describes a temperature-modulated localized reflectance probe which can be used in the method of the first embodiment. The temperature-modulated probe has a light introduction fiber and several light collection fibers. The light collection fibers are disposed at a short distance from the light introduction fiber. The maximum light source-detector distance is a center-center distance of less than 2 mm between the center of the light introduction fiber and the light collection fiber. By selecting the light source-detector distance of less than 2 mm, measurement of light signals generated from the upper skin layer without entrapping signals from adipose tissues or muscle tissues is surely carried out.

**[0051]** One aspect of the first embodiment is the use of a localized reflectance probe whose temperature has been set to a temperature substantially different from the normal temperature of the skin for collecting thermo-optical response signals. The temperature of the probe is maintained at a temperature substantially different from the normal temperature of the skin. A sudden temperature change upon contacting of the skin with the probe induces a change in glucose

metabolism in a nutrient capillary in the skin.

[0052] In still another aspect of the first embodiment, a glucose concentration is associated with a rate of change in effective attenuation coefficient according to a probe-skin contact time and a rate of oxygen consumption according to a probe-skin contact time. Accordingly, we represent the equation 7 as follows.

$$[G] = \sum_i [a_i * \{ (d\mu_{eff}/dt) \} \lambda_i] + \sum_j [b_j * (dOC/dt) r_j] \quad (8)$$

[0053] The sum of the first term ranges over a plurality of wavelengths ( $\lambda_i$ ) used, and the sum of the second term ranges over numerical values ( $r_j$ ) of the light source-detector distances used in the localized reflectance measurement. The term  $\mu_{eff}$  is an effective attenuation coefficient, which is associated with an absorption coefficient of a medium:  $\mu_a = 2303\epsilon C$  and a scattering coefficient of a medium:  $\mu'_s$  by the relational formula:  $\mu_{eff} = [(3\mu_a(\mu_a + \mu'_s))]^{1/2}$ .

[0054] The rate of change in oxygen consumption can be represented as a ratio of  $\mu_a$  at a wavelength at which absorption of deoxyhemoglobin is higher than that of oxyhemoglobin to  $\mu_a$  at a wavelength at which absorption of deoxyhemoglobin is lower than that of oxyhemoglobin. Table 1 shows  $\epsilon$  of oxyhemoglobin and deoxyhemoglobin, and calculated  $\mu_a$  values of two types of hemoglobin, the total hemoglobin at an oxygen saturation value of 95% and a total hemoglobin of 15 g/dL. Selected wavelengths were used in an apparatus for testing the first embodiment, and a large difference in  $\epsilon$  between two hemoglobin types is shown. Several wavelengths among these are shown in Table 1, and  $\epsilon$  and  $\mu_a$  of oxyhemoglobin and deoxyhemoglobin and the total hemoglobin are calculated with respect to a total hemoglobin concentration of 15 g/dL and an oxygen saturation value of 95% in Table 1.

[Table 1]

Table 1: Extinction coefficient and absorption coefficient of hemoglobin					
Wavelength nm	Total Hb (15 g/dL)	Oxyhemoglobin		Deoxyhemoglobin	
	$\mu_a$ (cm <sup>-1</sup> )	$\epsilon$	$\mu_a$ (cm <sup>-1</sup> )	$\epsilon$	$\mu_a$ (cm <sup>-1</sup> )
592	24.35	10468	21.59	25470	2.76
660	1.01	320	0.66	3227	0.35
880	2.58	1214	2.5	736	0.08
940	2.58	1214	2.5	693	0.08

[0055] When a pair of wavelengths in Table 1 is used, a rough estimate of a rate of change in oxygen consumption can be represented as follows.

$$d(OC)/dt = \alpha \{ d(\mu_a 660 / \mu_a 940) / dt \} \quad (9a)$$

$$d(OC)/dt = \beta \{ d(\mu_a 660 / \mu_a 880) / dt \} \quad (9b)$$

[0056] The latter functional form is similar to one to be used in the calculation of arterial oxygen saturation in heart beating, which is known as pulse oximetry.

Approximate formulae for scattering and absorption terms

[0057] The plotting of  $\ln(1/R(r_1))$  against  $\ln(R(r_1)/R(r_1))$  provides tracking of the interaction between an absorption coefficient and a scattering coefficient using a Monte Carlo grid. The plotting of  $\ln(1/R(r_1))$  against  $\ln(R(r_1)/R(r_1))$  at various time points in the probe/skin interaction provides a Monte Carlo-like grid, and its slope can be associated with an effective attenuation coefficient  $\mu_{eff}$ .

[0058] It is possible to roughly calculate a change in scattering coefficient and absorption coefficient with respect to a localized reflected light intensity ratio at a defined light source-detector distance and wavelength. A change in physical response can be expressed as follows.

$$\sum_i [a_i * \{ (d\mu_{eff}/dt) \} \lambda_i] = \sum_i [a_i * \{ d \ln(1/R_1) / d \ln(R_i/R_1) \} \lambda_i] \quad (10)$$

5

[0059] A change in physiological response can be expressed as follows.

$$\sum_j [b_j * (d(\mu_{a660}/\mu_{a940}/dt)) = \sum_j [b_j * \{ d \ln(R_{660}/R_{940}) / dt \} r_j] \quad (11)$$

10

[0060] Accordingly, a blood glucose concentration can be expressed as follows with respect to a localized reflected light intensity ratio at a defined light source-detector distance and wavelength.

15

$$[G] = \sum_i [a_i * \{ d \ln(1/R_1) / d \ln(R_i/R_1) \} \lambda_i] + \sum_j [b_j * \{ d \ln(R_{660}/R_{940}) / dt \} r_j] \quad (12)$$

20

[0061] Here,  $\lambda_i$  is 592, 660 or 880 nm, and  $r_j$  is a light source-detector distance. When the respective localization-reflectance signals are normalized to the initial time  $t_0$  sec in the same time window between  $t_n$  sec and  $t$  sec, the result is as follows.

25

$$[G] = \sum_i [a_i * \{ d \ln(1/R_1) / d \ln(R_i/R_1) \} \lambda_i] + \sum_j [b_j * \{ (\ln(R_{660}/R_{940})_t / \ln(R_{660}/R_{940})_{t_0}) r_j] \quad (13)$$

30

[0062] The first term in the equation (13) describes a change in both absorption and scattering coefficients. The scattering is dominant in the shortest light source-detector distance and a low absorption value. The absorption is dominant in the longest light source-detector distance and a high absorption value. This shall apply to the measurement at a hemoglobin absorption wavelength.

[0063] The metabolic effect of temperature on oxygen consumption will be described.

35

[0064] Another calculation for the method of the first embodiment in which  $\epsilon$  values of oxyhemoglobin and deoxyhemoglobin are used for deriving coefficients of oxygen consumption equation. The derived equation shows an association between a localized reflected light intensity at a defined light source-detector distance and wavelength and a ratio of a hemoglobin  $\epsilon$  value to a change in glucose concentration. We will start from the formula of  $\mu_a$  of the blood at a wavelength used in a measurement apparatus.

40

$$(\mu_a)_{592nm} \text{ at start} \approx \ln(R_{592})_0 = \epsilon C[\text{HbO}_2(0)] + \epsilon C[\text{Hb}(0)], \text{ at } 592 \text{ nm} \quad (14)$$

45

$$(\mu_a)_{592nm} \text{ at } t \text{ sec} \approx \ln(R_{592})_t = \epsilon C[\text{HbO}_2(t)] + \epsilon C[\text{Hb}(t)], \text{ at } 592 \text{ nm} \quad (15)$$

50

$$(\mu_a)_{592nm} \text{ at start} \approx \ln(R_{592})_0 = 10,468 * C[\text{HbO}_2(0)] + 25,470 * [\text{Hb}(0)] \quad (16)$$

55

$$(\mu_a)_{592\text{nm}} \text{ at } t \text{ sec} \approx \text{Ln}(R_{592})_t =$$

$$10,468 * C[\text{HbO}_2(t)] + 25,470 * [\text{Hb}(t)] \quad (17)$$

[0065] A similar equation can be written for other wavelengths of 660, 880 and 940 nm. By subtracting the equation (16) from the equation (17), a change in the absorption coefficient at 592 nm is shown as follows as a result of temperature jump.

$$\Delta(\mu_a)_{592\text{nm}} \approx \text{Ln}[(R_{592})_t / (R_{592})_0] =$$

$$10,468 * \Delta C[\text{HbO}_2] + 25,470 * \Delta C[\text{Hb}] \quad (18)$$

[0066]  $\Delta C[\text{HbO}_2]$  is a change in  $\text{HbO}_2$  concentration induced by temperature, which generates oxygen necessary for temperature-induced glycolysis. A similar equation is applied to other wavelengths, and the equations (19) to (21) are provided.

$$\Delta(\mu_a)_{660\text{nm}} \approx \text{Ln}[(R_{660})_t / (R_{660})_0] = 320 * C[\text{HbO}_2] +$$

$$3,227 * C[\text{Hb}] \quad (19)$$

$$\Delta(\mu_a)_{880\text{nm}} \approx \text{Ln}[(R_{880})_t / (R_{880})_0] = 1,214 * C[\text{HbO}_2] +$$

$$673 * C[\text{Hb}] \quad (20)$$

$$\Delta(\mu_a)_{940\text{nm}} \approx \text{Ln}[(R_{940})_t / (R_{940})_0] = 1,214 * C[\text{HbO}_2] +$$

$$6,934 * C[\text{Hb}] \quad (21)$$

[0067] By multiplying the equation (21) by 36.75, the equations (18) and (21) are solved with respect to  $C[\text{HbO}_2]$ , and the equation (22) is provided.

$$36.75 * \text{Ln}[(R_{940})_t / (R_{940})_0] = 36.75 * \times$$

$$1,214 * C[\text{HbO}_2] + 25,470 * C[\text{Hb}] \quad (22)$$

[0068] The equation (22) is subtracted from the equation (18).

$$\{36.75 * \text{Ln}[(R_{940})_t / (R_{940})_0] - \text{Ln}[(R_{592})_t / (R_{592})_0]\} =$$

$$34,150 * \Delta C[\text{HbO}_2] \quad (23)$$

[0069] The equation is solved with respect to  $\Delta C[\text{HbO}_2]$ .

$$\Delta C[\text{HbO}_2] = (2.928 * 10^{-5}) * \{36.75 * \text{Ln}[(R_{940})_t /$$

$$(R_{940})_0] - \text{Ln}[(R_{592})_t / (R_{592})_0]\} \quad (24)$$

[0070] By solving the equation with respect to 880 nm and 592 nm, the following equation is provided.

$$\Delta C[\text{HbO}_2] = (2.928 \times 10^{-5}) * \{36.75 * \text{Ln}[(R_{880})_t / (R_{880})_0] - \text{Ln}[(R_{592})_t / (R_{592})_0]\} \quad (25)$$

[0071] In the embodiment of the first embodiment, a change in the molar concentration of glucose by excess glycolysis,  $\Delta[G]$ , is associated with  $\Delta C[\text{HbO}_2]$ .

$$\Delta[G] \propto 2.928 \times 10^{-5} * \{36.75 * \text{Ln}[(R_{940})_t / (R_{940})_0] - \text{Ln}[(R_{592})_t / (R_{592})_0]\} \quad (26)$$

[0072] In order to convert  $\Delta[G]$  from a mole unit to mg/dl, it is multiplied by  $1.8 \times 10^4$ .

$$\Delta[G] \propto \Delta C[\text{HbO}_2] \propto F(\text{OC})_1 = 0.527 * \{36.75 * \text{Ln}[(R_{940})_t / (R_{940})_0] - \text{Ln}[(R_{592})_t / (R_{592})_0]\} \quad (27)$$

[0073]  $F(\text{OC})_1$  is a function representing oxygen consumption from localization-reflectance optical measurement at 592 nm and 940 nm.

[0074] According to the following same steps, it is possible to calculate the oxygen consumption function,  $F(\text{OC})_2$ , from the reflectances measured at 660 nm and 940 nm.

[0075] By multiplying the equation (21) by 4.6566, the equations (19) and (21) are solved with respect to  $\Delta C[\text{HbO}_2]$ , and the equation (28) is provided.

$$4.6566 * \text{Ln}[(R_{940})_t / (R_{940})_0] = 5,653 * \Delta C[\text{HbO}_2] + 3,227 * C[\text{Hb}] \quad (28)$$

[0076] The equation (19) is subtracted from the equation (28).

$$\{4.969 * \text{Ln}[(R_{940})_t / (R_{940})_0] - \text{Ln}[(R_{660})_t / (R_{660})_0]\} = 5,621 * \Delta C[\text{HbO}_2] \quad (29)$$

$$\Delta C[\text{HbO}_2] = (1/5621) * \{4.6566 * \text{Ln}[(R_{940})_t / (R_{940})_0] - \text{Ln}[(R_{660})_t / (R_{660})_0]\} \quad (30)$$

$$\Delta C[\text{HbO}_2] = 1.779 \times 10^{-4} * \{4.6566 * \text{Ln}[(R_{940})_t / (R_{940})_0] - \text{Ln}[(R_{660})_t / (R_{660})_0]\} \quad (31)$$

[0077] In the embodiment of the invention,  $\Delta C[\text{HbO}_2]$  has a correlation with  $\Delta[\text{glucose}]$ ,  $\Delta[G]$ , and a change in the molar concentration of glucose by excess glycolysis caused as a result of thermal stimulation is proportional to  $\Delta C[\text{HbO}_2]$  in the same manner as the case of the equation (26).

$$\Delta[G] \propto 1.779 \times 10^{-4} * \{ 4.6566 * \ln [ (R_{940})_t / (R_{940})_0 ] - \ln [ (R_{660})_t / (R_{660})_0 ] \} \quad (32)$$

**[0078]** In order to convert the concentration of  $\Delta[G]$  from a mole unit to mg/dl, it is multiplied by  $1.8 \times 10^4$ .

$$\Delta[G] \propto \Delta C \{ \text{HbO}_2 \} \propto F(\text{OC})_2 = 3.2022 * \{ 4.6566 * \ln [ (R_{940})_t / (R_{940})_0 ] - \ln [ (R_{660})_t / (R_{660})_0 ] \} \quad (33)$$

**[0079]**  $F(\text{OC})_2$  is a function representing oxygen consumption from localization-reflectance optical measurement at 660 nm and 940 nm. The oxygen consumption functions,  $F(\text{OC})_1$  and  $F(\text{OC})_2$ , are conceptually similar to each other, but can have different values depending on a skin structural effect.

**[0080]** An equation obtained by generalizing the equations representing a glucose concentration with respect to a change in all the attenuation coefficients and oxygen consumption functions is as follows.

$$[G] = a_0 + \sum_i [a_i * \{ d \ln(1/R_1) / d \ln(R_i/R_1) \} \lambda_i] + \sum_j [b_j * \{ F(\text{OC})_1 \} r_j] + \sum_k [b_k * \{ F(\text{OC})_2 \} r_k] \quad (34)$$

**[0081]** Various modifications of this equation and various determination criteria for the range of variables in the equation can be used.

Time window for calculation

**[0082]** The calculation method of this embodiment includes the step of calculating a rate of change in localized reflectance values at a plurality of wavelengths and light source-detector distances. In a modification example of the first embodiment, the calculation method includes the step of calculating a degree of change in at least one parameter associated with the time dependent effect of the temperature stimulation on the localized reflectance values at a plurality of wavelengths and light source-detector distances. The degree of change is calculated for at least one time window and is averaged over adjacent time windows. The time window for calculation starts after the skin-probe adaptation.

Advantage of this embodiment

**[0083]** This embodiment is different from the prior art in several aspects. In the first embodiment, temperature-induced glycolysis is tracked by inducing a temperature change in the human skin, measuring localized reflectance signals at several defined light source-detector distances, and correlating functions derived from the reflectance values at a plurality of wavelengths and light source-detector distances with a glucose concentration.

**[0084]** US Patent Nos. 5795305 and 5924996, US Patent Application Publication No. 2005/0124868 and European Patent Application Publication No. 1537822 did not take the skin-probe adaptation effect on the optical and thermal signals into consideration, and did not induce a temperature change that affects glucose metabolism. US Patent No. 5978691 does not disclose the measurement of oxygen consumption as a result of the physiological effect of glucose metabolism or the use of temperature-enhanced glucose metabolism, or does not take the time window for reducing the tissue-probe adaptation effect on the measurement to the minimum into consideration. In US Patent No. 5978691, a temperature-induced change in the hemoglobin equilibrium is measured. The method includes measurement of diffuse reflectance or transmission. This does not specify a defined light source-detector distance, and thus does not specify a depth in a tissue.

**[0085]** In the method and apparatus of this embodiment, a time for adaptation of the skin to the measurement probe is set, and signals to be measured over a specific time window, in which the skin-probe interaction effect on the signals is reduced to the minimum are used. US Patent No. 5785305, US Patent No. 5924996 and US Patent No. 5978691 do not set a time for adaptation of the measurement probe to the skin or do not use signals to be measured over a specific time window, in which the skin-probe adaptation effect on the signals is reduced to the minimum.

**[0086]** The main feature of this embodiment is as follows:

- a. the step of measuring a change in localized reflectance according to time at a wavelength corresponding to light absorption by oxyhemoglobin and deoxyhemoglobin and calculating functions associated with a change in oxygen consumption;
- b. the step of selecting a time window in which a tissue-probe adaptation effect on a signal is reduced to the minimum; and
- c. the step of deriving a calibration relationship between a combination of these oxygen consumption functions and a glucose concentration, and using the resulting calibration relationship for predicting a glucose concentration in the body are included.

**[0087]** FIG. 1 shows an apparatus for noninvasive measurement of glucose according to this embodiment. FIG. 2 shows a specific structure of a measurement head (also referred to as a probe) of the apparatus for noninvasive measurement of glucose of FIG. 1. A temperature control pack 1 includes a thermoelectric module 2 as a heat generator and a pad 3 which is contacted with the skin of a subject. The heating value of the thermoelectric module 2 is modulated by a temperature controller 4. Further, the temperature modulation operation of the temperature controller 4 is under the control of a computer 5. The computer 5 controls the temperature modulation and also plays a role in controlling the operating procedure of the method for noninvasive measurement of glucose according to this embodiment and operating the respective steps. In a central portion of the control pack 1, a tubular opening is formed and optical fibers 8 and 9 are inserted therein. To the optical fiber 8, a light source 6 is optically connected, and to the optical fibers 9, a light detector (signal detector) 7 is optically connected. Between the light source 6 and the optical fiber 8, a beam splitter 11 is disposed, and a part of light from the light source 6 is introduced into a reference detector 12.

**[0088]** The optical fiber 8 is disposed in the center, and the optical fibers 9 are arranged around the optical fiber 8 at short intervals. The maximum distance between the optical fiber 8 and the optical fibers 9 is less than 2 mm. That is, the optical fibers 8 and 9 are bundled within an area in a substantially circular shape with a diameter of 4 mm. A relationship between the wavelength of the localized reflectance probe and the distance between the light source 6 and the detector 7 is shown in Table 2. As described in US Patent No. 6654620, one drop of silicone oil is applied to the skin of a subject and then wiped off to leave a very thin layer of oil on the skin, whereby the thermal conductivity is enhanced.

[Table 2]

Table 2: Wavelength and source-detector distance			
Wavelength nm		Source-detector distance mm	
$\lambda_1$	592	$r_1$	0.559
$\lambda_2$	660	$r_2$	0.879
$\lambda_3$	880	$r_3$	1.318
$\lambda_4$	940	$r_4$	1.758

Calculation of oxygen consumption and change in attenuation coefficient

**[0089]** FIG. 3 shows the response of the skin of a diabetic patient to an optical probe at 40°C pressed against the skin of the forearm of the subject. The functions of oxygen consumption are calculated as follows using modification of the equation 9.

$$d(OC)/dt = \gamma * F(OC) = \frac{1000 * \ln(R_{660}/R_{940})_t}{\ln(R_{660}/R_{940})_5 \text{ sec}} \quad (9c)$$

**[0090]** In the equation, R represents a localized reflectance at each light source-detector distance. The signals were normalized to signals at 5 sec intervals.

**[0091]** The calculated F(OC) increases when the probe at 40°C is brought into contact with the skin, and then, reaches an asymptotic value after about 120 sec. The thermal modeling (J. Biomedical Optics., 2003; 8, 191-205) shows that when the probe came into contact with the skin, the temperature up to a depth of 2 mm reached an equilibrium after 120 sec. F(OC) increases at all the light source-detector distances. The order of the increase in F(OC) is as follows.

$$F(OC) r_4 > F(OC) r_3 > F(OC) r_2 > F(OC) r_1$$

[0092] The maximum change in F(OC) occurs at initial 90 sec. As shown in FIG. 4, F(OC) value has a linear relationship with the skin-probe contact time.

[0093] Table 3 shows the results of calculation of functions of oxygen consumption at various light source-detector distances from the data of FIG. 4.

[Table 3]

Table 3: Calculation of functions of oxygen consumption at various distances		
Source-detector distance mm	Probe at 40°C	
	Fitting equation	Correlation coefficient (r <sup>2</sup> )
0.559	F(OC) = 0.1363 t(s) + 1.0477	0.91
0.879	F(OC) = 0.1925 t(s) + 1.0512	0.91
1.318	F(OC) = 0.3114 t(s) + 0.5772	0.93
1.758	F(OC) = 0.4498 t(s) + 3.7338	0.92

[0094] As shown in Table 3, the calculated functions of oxygen consumption linearly change with the time of probe-skin interaction at four light source-detector distances over the measured time window.

[0095] A rough estimate of a rate of change in effective attenuation coefficient at each wavelength according to the probe-skin contact can be achieved by plotting the values of Ln(R<sub>4</sub>/R<sub>1</sub>) at the respective wavelengths against time and calculating the slope.

[0096] FIG. 5 shows the plot of Ln(R<sub>4</sub>/R<sub>1</sub>) against time with respect to a probe heated to 40°C. Lozenges indicate 592 nm, circles indicate 660 nm, Xs indicate 880 nm, and triangles indicate 940 nm. Table 4 shows the results of calculation of approximate μ<sub>eff</sub> represented by Ln(R<sub>4</sub>/R<sub>1</sub>) and calculated at various wavelengths from the data of FIG. 5.

[Table 4]

Table 4: Approximate μ <sub>eff</sub> at various wavelengths		
Wavelength nm	Probe at 40°C	
	Fitting equation	Correlation coefficient (r <sup>2</sup> )
592	Ln(R <sub>4</sub> /R <sub>1</sub> ) = -1.5 × 10 <sup>-3</sup> t(s) + 0.0088	0.96
660	Ln(R <sub>4</sub> /R <sub>1</sub> ) = +5.0 × 10 <sup>-5</sup> t(s) + 0.0021	0.15
880	Ln(R <sub>4</sub> /R <sub>1</sub> ) = -0.3 × 10 <sup>-3</sup> t(s) + 0.0013	0.98
940	Ln(R <sub>4</sub> /R <sub>1</sub> ) = -0.3 × 10 <sup>-3</sup> t(s) + 0.0013	0.98

[0097] The approximate μ<sub>eff</sub> represented by Ln(R<sub>4</sub>/R<sub>1</sub>) and calculated at various wavelengths changes linearly with the contact time in a time window between 5 and 90 sec except for the wavelength of 600 nm showing the smallest slope and low r<sup>2</sup>. The slope approximates to μ<sub>eff</sub> and changes in the following order.

$$\text{Ln}(R_4/R_1)_{592\text{nm}} > \text{Ln}(R_4/R_1)_{880\text{nm}} =$$

$$\text{Ln}(R_4/R_1)_{940\text{nm}} >> \text{Ln}(R_4/R_1)_{660\text{nm}}$$

[0098] A change in the slope is similar to a change in the extinction coefficient reported at various wavelengths, ε(HbO<sub>2</sub>) or μ<sub>a</sub>(HbO<sub>2</sub>), however, 660 nm which provides the smallest value of ε(HbO<sub>2</sub>) is excluded. This shows that a change in light absorption is the dominant contributor to be reflected light intensity.

Degree of signal change and use of moving average of signal change

[0099] The degree of change F(OC) is averaged over several adjacent time regions by using a moving average calculation. FIG. 6 shows simulation of profile of change in oxygen consumption rate when the skin is contacted with a probe heated such that the temperature thereof is increased by about 10°C. The 4-point moving average regions include data between 15 and 30 sec, time regions between 20 and 35 sec, 25 and 40 sec, and 30 and 45 sec. These time regions are used when the data of an embodiment 8 is analyzed.

Blood glucose concentration and clinical correlation

[0100] A clinical study was carried out in a hospital for diabetic patients who accepted treatment and signed informed consent. The ethical committee approved the study procedure. The testing time lasted 3 to 5 days. Each patient performed the test several times a day by using a NI apparatus and a home glucometer. The patients maintained daily activities and a therapeutic regimen. The data of 6 patients analyzed by using the modification of the equation 34 are shown in Table 5, however, in Table 5, an inclusion standard for data points in the subsequent calculation is included. The inclusion standard was as follows. a)  $d(OC)/dt < 0$ , b)  $dLn(R_{592})/dt < 0$ , c)  $dLn(R_{880})/dt < 0$

[Table 5]

Table 5: Inclusion standard for using change in scattering and oxygen consumption		
Equation No.	Fitting equation	Inclusion standard
34a	$[G] = a_0 + a_1 * \{d[Ln(R_4/R_1)]/dt\}_{592 \text{ nm}} + a_2 * \{d[Ln(R_4/R_1)]/dt\}_{880 \text{ nm}} + a_3 * [d(OC)/dt]_{r_2} + a_5 * [d(OC)/dt]_{r_3}$	a, b, c
34b		a, b, $-0.8 < dLn(R_{880})/dt < 0.3$
34c		a, b, $-1.0 < dLn(R_{880})/dt < +1.0$
34d	$[G] = a_0 + a_1 * \{d[Ln(R_4/R_1)]/dt\}_{592 \text{ nm}}$	B
34e	$[G] = a_0 + a_1 * \{d[Ln(R_4/R_1)]/dt\}_{880 \text{ nm}}$	$-0.8, dLn(R_{880})/dt < +0.3$
34f	$[G] = a_0 + a_1 * \{d[Ln(R_4/R_1)]/dt\}_{880 \text{ nm}}$	$-1.0, dLn(R_{880})/dt < +1.0$
34g	$[G] = a_0 + a_1 * \{d[Ln(R_4/R_1)]/dt\}_{592 \text{ nm}} + a_2 * \{d[Ln(R_4/R_1)]/dt\}_{880 \text{ nm}}$	b, $0.8 < dLn(R_{880})/dt < +0.3$
34h		b, $-1.0 < dLn(R_{880})/dt < +1.0$
34i	$[G] = a_0 + a_3 * [d(OC)/dt]_{r_2}$	A
34j	$[G] = a_0 + a_5 * [d(OC)/dt]_{r_3}$	A
34k	$[G] = a_0 + a_3 * [d(OC)/dt]_{r_2} + a_5 * [d(OC)/dt]_{r_3}$	A
34l	$[G] = a_0 + a_1 * \{d[Ln(R_4/R_1)]/dt\}_{592 \text{ nm}} + a_3 * [d(OC)/dt]_{r_2} + a_4 * [d(OC)/dt]_{r_3}$	a, b
34m	$[G] = a_0 + a_2 * \{d[Ln(R_4/R_1)]/dt\}_{880 \text{ nm}} + a_3 * [d(OC)/dt]_{r_2} + a_4 * [d(OC)/dt]_{r_3}$	a, $-0.8 < dLn(R_{880})/dt < +0.3$

(continued)

Equation No.	Fitting equation	Inclusion standard
34n	$[G] = a_0 + a_2 \cdot \{d[\ln(R_4/R_1)]/dt\}_{880 \text{ nm}} + a_3 \cdot [d(OC)/dt]_{r_2} + a_4 \cdot [d(OC)/dt]_{r_3}$	$a, -1.0 < d\ln(R_{880})/dt < +1.0$

**[0101]** A linear least square regression analysis was used for constructing pentanomial, tetranomial, trinomial, and binomial regression models in combinations of calculated oxygen consumption, calculated attenuation functions, and noninvasively measured glucose concentrations. The calibrated standard error and calibrated correlation coefficient were determined with respect to the respective first days of a study. The constructed models were used for predicting a glucose concentration from a data point at a later date. The data of the respective patients were separately processed. The calculated calibration points and prediction points were plotted on a Clarke Error Grid scatter diagram using a modification of the equation 34. The Clarke Error Grid is commonly used for showing the distribution of predicted glucose values in various zones of plots, and the respective zones of plots have a special clinical significance in predicted intervention.

[Table 6]

Equation No.	Number of terms	Type of term: constant +	n	r <sub>c</sub>	SEC mg/dl	r <sub>p</sub>	SEP mg/dl
34a	5	2 μ <sub>eff</sub> + 2 OC	39	0.81	45.4	0.44	123.0
34b	5	2 μ <sub>eff</sub> + 2 OC	39	0.81	44.5	0.34	118.4
34c	5	2 μ <sub>eff</sub> + 2 OC	42	0.81	44.3	0.28	146.4
34d	2	μ <sub>eff</sub>	43	0.74	50.4	0.73	60.3
34e	2	μ <sub>eff</sub>	40	0.7	53.7	0.71	64
34f	2	μ <sub>eff</sub>	43	0.7	49.7	0.72	62.4
34g	3	2 μ <sub>eff</sub>	40	0.75	49.7	0.72	62.4
34h	3	2 μ <sub>eff</sub>	43	0.75	49.4	0.72	61.6
34i	2	OC	41	0.74	51.2	0.74	60.4
34j	2	OC	42	0.74	50.5	0.72	61.7
34k	3	2 OC	42	0.76	49.3	0.72	62.8
34l	4	μ <sub>eff</sub> + 2 OC	42	0.8	45.8	0.69	66.1
34m	4	μ <sub>eff</sub> + 2 OC	39	0.77	48.1	0.71	65.2
34n	4	μ <sub>eff</sub> + 2 OC	42	0.77	47.9	0.68	66

**[0102]** The five-term equations 34a, 34b and 34c (constant term + 2 attenuation coefficient terms + 2 OC terms) show the evidence of overfitting. The equations 34d, 34e and 34f are a two-term equation (constant term + attenuation coefficient term) based on various wavelengths and the inclusion criteria. All have good calibration and prediction parameters, and distribution in the A and B zones of the Clarke Error Grid. The attenuation coefficient term at 592 nm (the highest absorbance for hemoglobin) has the best correlation parameters. A combination of all two attenuation terms at 592 and 880 nm provides the three-term equations 34g and 34h, which results in improving the two-term equations 34d, 34e and 34f.

**[0103]** The use of OC term is shown in the equations 34i to 34k. The equations 34i and 34j are a two-term equation, and 34k is a three-term equation having two OC terms. The data shown in Table 6 shows the calibration and prediction capability of three OC models. By adding a μ<sub>eff</sub> term to the equation 34k, the equations 34l, 34m and 34n are provided.

## EP 2 243 425 B1

All these three models result in giving a slight improvement of calibration to 34k. The time window in which this calculation is performed extended from 5 sec to 60 sec from the probe-skin interaction.

Selection of optimal time interval

5

**[0104]** In this embodiment, the equation 34k was applied to an analysis of 6 patients. The equation 34k is a three-term model consisting of a constant term and two OC terms. The data on day 1 and day 2 were used in a calibration set. The data point on day 3 was used as a prediction set for each patient. A cumulative Clarke Error Grid was constructed for data points of all the patients, and overall calibration and prediction parameters were calculated. Ten time intervals were selected from 5 sec to 60 sec of the probe-skin interaction windows and as a result, time intervals between 55 sec and 30 sec were provided. The number of time points in the selected intervals is between 12 and 7. The calculation results are shown in Table 7.

10

**[0105]** The results in Table 7 show that the use of a time interval between 30 sec and 60 sec consequently provides a better calibration and prediction result. Because data was used in calculation, the use of a delay time of 30 sec from the initiation of the probe-skin contact reduced the contribution of skin-probe adaptation to correlation to the minimum, therefore, it had the best correlation with glucose.

15

[Table 7]

Equation	Start/finish time (sec)	$\Delta t$ (sec)	n	$r_c$	SEC	$r_p$	SEP
34k-0	5/60	55	12	0.75	51.0	0.74	62.9
34k-1	10/60	50	11	0.76	49.3	0.72	62.8
34k-2	15/60	45	10	0.78	47.7	0.69	66.3
34k-3	20/60	40	9	0.78	47.2	0.7	63.4
34k-4	25/60	35	8	0.78	47.1	0.75	62.5
34k-5	30/60	30	7	0.80	45.6	0.83	59.0
34k-6	5/55	50	11	0.75	52.2	0.73	69
34k-7	10/55	45	10	0.76	48.8	0.72	61.6
34k-8	15/55	40	9	0.77	46.7	0.70	64.7
34k-9	20/55	35	8	0.8	44.9	0.7	67.5
34k-10	20/55	30	7	0.82	42.5	0.72	69.0

20

25

30

35

40

**[0106]** A similar result was obtained when the equation 341 which is a four-term model including a  $\mu_{eff}$  term at 592 nm and two OC terms was used. The equation 34m is also a four-term model including a  $\mu_{eff}$  term at 880 nm and two OC terms. It was shown by calculation that the use of a time interval between 30 sec and 60 sec consequently provides a better calibration and prediction model whether a three-term model is used or a four-term model is used. The use of a time interval of 30 sec reduces the contribution of skin-probe adaptation to correlation to the minimum.

45

**[0107]** The time intervals were from 30 to 60 sec, however, 7 data points are used in calculation of rates. The overall prediction correlation coefficient values are higher than those shown in Table 6, in which a complete time window ranging from 5 to 60 sec was used in calculation.

50

[Table 8]

Equation	$r_c$	SEC	$r_p$	SEP	% in A + B zone	% in C + D zone	% in E zone
34k-5	0.80	45.6	0.83	59.0	94.7	5.3	0
341-5	0.86	39.4	0.80	58.6	94.7	5.3	0
34m-5	0.76	48.8	0.72	61.6	94.4	5.6	0

55

[0108] In this embodiment, models consisting of various three terms of oxygen consumption only were attempted.

[0109] Generalized equation is as follows.

$$[G] = a_0 + a_1 * [F(OC)_n @ r_i - F(OC)_n @ r_j] + a_2 * [F(OC)_m @ r_i - F(OC)_m @ r_j] \quad (35)$$

[0110] The functions of F(OC)<sub>1</sub> and F(OC)<sub>2</sub> were defined as follows before.

$$F(OC)_1 = 0.527 * \{ 36.75 * \ln [ (R_{940})_t / (R_{940})_0 ] - \ln [ (R_{592})_t / (R_{592})_0 ] \} \quad (27)$$

$$F(OC)_2 = 3.2022 \{ 4.6566 \ln [ (R_{940})_t / (R_{940})_0 ] - \ln [ (R_{660})_t / (R_{660})_0 ] \} \quad (33)$$

[0111] A three-term model in which a combination of F(OC)<sub>1</sub> and F(OC)<sub>2</sub> at different light source-detector distances is used provides the following equation.

$$[G] = a_0 + a_1 * [F(OC)_1 @ r_2 - F(OC)_1 @ r_1] + a_2 * [F(OC)_2 @ r_2 - F(OC)_2 @ r_1] \quad (36)$$

[0112] Four oxygen consumption functions were calculated, however, the fitting equations have only three terms. When a combination of each of two OC functions at various light source-detector distances are used, the number of terms in the fitting equations is reduced from five to three, which reduces the possibility of constructing an overfitting line of data to the minimum. Various modifications of the equation 36 are as follows.

$$[G] = a_0 + a_1 * F(OC)_1 @ r_1 - a_2 * F(OC)_1 @ r_2 \quad (37)$$

$$[G] = a_0 + a_1 * F(OC)_2 @ r_1 - a_2 * F(OC)_2 @ r_2 \quad (38)$$

$$[G] = a_0 + a_1 * [F(OC)_1 @ r_2 - F(OC)_1 @ r_1] + a_2 * [F(OC)_2 @ r_2 - F(OC)_2 @ r_1] \quad (39)$$

$$[G] = a_0 + a_1 * [F(OC)_1 @ r_2 - F(OC)_1 @ r_1] + a_2 * [F(OC)_2 @ r_2 - F(OC)_2 @ r_1] \quad (40)$$

[0113] These equations were used for analyzing data for the patient 1001. The OC function is a logarithmic function, therefore, two subtractions as the case of a term of difference between two OC terms in (37) and (38) and F(OC)<sub>1</sub> and F(OC)<sub>2</sub> in the equation 40 represents a ratio term of a localized reflectance ratio at two light source-detector distances.

[0114] The data points of patients were collected in a period of 7 days. 16 out of 30 data points were passed the inclusion criteria. An average of 4 × 15 sec regions of time response as described above was used. In the calibration, 12 data points from day 1 to day 3 in the clinical study were used, and in the prediction, 4 data points from day 5 to day 7 in the clinical study were used. The results are shown in FIG. 7A to FIG. 7D.

[0115] The equation 37 is a three-term equation including a constant and a difference between two  $F(OC)_1$  terms. The regression coefficient in the equation 37 is as follows.

$$[G] = 195.2 + 432.3 * F(OC)_1 @ r_1 - 391.6 * F(OC)_1 @ r_2 \quad (37a)$$

[0116] The data are plotted on FIG. 7A. The calibration and prediction parameters are good as shown in Table 9. The four predicted glucose values fall in the A zone of the Clarke Error Grid. As shown in Table 10, by linearly approximating the four predicted glucose values to the measured glucose values, an equation:  $r^2 = 0.19$  is generated.

[0117] In still another embodiment, the equation 38 was used for analyzing the data of a subject No. 1001. The three-term approximate linear equation 38, the coefficients  $a_0$ ,  $a_1$  and  $a_2$  obtained by calibration of two variables are provided in the equation 38a.

$$\text{Glucose} = 167.9 + 7351.3 * F(OC)_2 @ r_1 - 7985.2 * F(OC)_2 @ r_2 \quad (38a)$$

[0118] The data are plotted on FIG. 7B. The calibration and prediction parameters are good as shown in Table 9. The four predicted glucose values fall in the A zone of the Clarke Error Grid. As shown in Table 10, by linearly approximating the four predicted glucose values to the measured glucose values, a high correlation function:  $r^2 = 0.75$  is generated. The use of  $F(OC)_2$  consequently provides a better correlation with respect to this patient.

[0119] In still another embodiment, the equation 39 was used for analyzing the data of a subject No. 1001. The three-term approximate linear equation 39, the coefficients  $a_0$ ,  $a_1$  and  $a_2$  obtained by calibration of two variables are provided in the equation 39a.

$$[G] = 178.7 + 115.2 * (F(OC)_1 @ r_2 - F(OC)_1 @ r_1) - 8303.9 * (F(OC)_2 @ r_2 - F(OC)_2 @ r_1) \quad (39a)$$

[0120] The data are plotted on FIG. 7C. The calibration and prediction parameters are good as shown in Table 9. The four predicted glucose values fall in the A zone of the Clarke Error Grid. As shown in Table 10, by linearly approximating the four predicted glucose values to the measured glucose values, a high correlation function:  $r^2 = 0.75$  is generated.

[0121] FIG. 7D shows the use of the equation 40 for analyzing the data of a subject No. 1001. The equation 40 is a three-term approximate linear equation including a constant, a difference between two  $F(OC)_1$  terms and a sum of two  $F(OC)_1$  terms. The first parenthesis is a difference between two  $F(OC)_1$  values which consequently provide localized reflectance ratios at two light source-detector distances  $r_1$  and  $r_2$ . The second term in the parenthesis is a sum of two  $F(OC)_2$  values which consequently provide a multiplication. The three-parameter approximate linear equation, the coefficients  $a_0$ ,  $a_1$  and  $a_2$  obtained by calibration of two variables are provided in the equation 40a.

$$[G] = 154 - 529.8 * (F(OC)_1 @ r_2 - F(OC)_1 @ r_1) - 1351 * (F(OC)_2 @ r_2 - F(OC)_2 @ r_1) \quad (40a)$$

[Table 9]

Table 9: Linear least squares calibration and prediction parameters in three-term oxygen consumption model						
Equation/FIG.	Calibration			Prediction		
	Number of data points = 12 Average [G] = 217.7 mg/dl			Number of data points = 4 Average [G] = 203.8 mg/dl		
	$r_c$	SEC	SEC%	$r_p$	SEP	SEP%
37/FIG. 7A	0.44	48.1	22.1	0.94	15.9	7.8
38/FIG. 7B	0.86	27	12.4	0.95	40.2	19.7
39/FIG. 7C	0.87	26.7	12.3	0.95	38	18.6
40/FIG. 7D	0.51	46	21.1	0.96	19.3	9.5

[0122] As shown in Table 9, the equations 38 and 39 provide the best calibration parameters and good prediction parameters.

[Table 10]

Table 10: Linear relationship between noninvasively predicted glucose values (Y) and reference glucose values (X)		
Regression model	Y = ax + b	Correlation coefficient $r^2$
Equation 37/FIG. 7A	Y = 0.1909x + 176.06	0.1909
Equation 38/FIG. 7B	Y = 0.7455x + 55.367	0.7455
Equation 39/FIG. 7C	Y = 0.7502x + 54.323	0.7502
Equation 40/FIG. 7D	Y = 0.2593x + 161.26	0.2593

[0123] The use of three terms (a constant term + two oxygen consumption terms) derived calibration and prediction models of a change in glucose concentration in a diabetic patient over a period of 7 days. Oxygen consumption is calculated at two light source-detector distances in the localized reflectance measurement. This embodiment is directed to calibration of one patient. The coefficients in the model or the types of OC functions depend on a disease condition, a type of drug used by a patient, and a diabetic period, and vary depending on a patient.

[0124] In this connection, the present invention is not limited to the above embodiment as such, and may be embodied in implementation phase by codifying the components without departing from the scope of the invention. Further, various inventions can be created by appropriately combining the plurality of components disclosed in the above embodiment. For example, several components may be eliminated from all the components disclosed in the embodiment.

Industrial Applicability

[0125] According to the present invention, in a method for noninvasive measurement of glucose and an apparatus for noninvasive measurement of glucose, a temperature change is induced in the human skin, localized reflectance signals at several defined light source-detector distances are measured, and functions derived from the reflectance values at a plurality of wavelengths and light source-detector distances are correlated with a glucose concentration, whereby temperature-induced glycolysis can be tracked.

Claims

1. A method for noninvasive measurement of glucose using a reflected light intensity which changes according to light scattering and light absorption by a hemoglobin variant as a biological index with a strong color, comprising the steps of:

bringing a localized reflectance optical probe whose temperature has been modulated to a temperature substantially different from the normal temperature of the skin into contact with the skin for inducing a change in glucose metabolism in a nutrient capillary in the skin and changing the concentration of a hemoglobin variant

as the change in glucose metabolism;  
 selecting a time window for data collection in which a tissue-probe adaptation effect on the resulting signal is small;  
 measuring a change in localized reflected light signals with respect to various light source (6)-detector (7)  
 distances, various wavelengths and various contact times during a specified time from the contact of the probe  
 with the skin;  
 calculating a change in at least one function associated with the effect of thermal stimulation on a change in  
 light absorption by hemoglobin as a result of the effect of temperature on glucose metabolism;  
 calculating a change in at least one function associated with the effect of thermal stimulation on a change in  
 light attenuation as a result of a change in light scattering and blood flow;  
 deriving a calibration relationship between a combination of the calculated functions derived from the localized  
 reflectance signals and a glucose concentration; and  
 using the measurement and the established calibration relationship for predicting a glucose concentration in a  
 subject at a subsequent time,  
 wherein the calculation step includes the step of calculating a degree of change in light absorption as a function  
 associated with the time dependent effect of the temperature on the localized reflectance values at a plurality  
 of wavelengths and light source (6)-detector (7) distances, in which the degree of change is calculated for at  
 least one time window, **characterized in that** the degree of change in light absorption is averaged over at least  
 two adjacent time windows using a moving average calculation.

2. The method according to claim 1, wherein the maximum light source (6)-detector (7) distance in the localized  
 reflectance probe is 2 mm or less.

3. An apparatus for noninvasive measurement of glucose, which uses a reflected light intensity that changes according  
 to light scattering and light absorption by a hemoglobin variant as a biological index with a strong color, comprising  
 a unit (2) which modulates the temperature of a localized reflectance optical probe, which has been brought into  
 contact with the skin for inducing a change in glucose metabolism in a nutrient capillary in the skin and changing  
 the concentration of a hemoglobin variant as the change in glucose metabolism, to a temperature substantially  
 different from the normal temperature of the skin;

a unit which selects a time window for data collection in which a tissue-probe adaptation effect on the resulting  
 signals is small;

a unit which measures a change in localized reflected light signals with respect to various light source (6)-detector  
 (7) distances, various wavelengths and various contact times during a specified time from the contact of the probe  
 with the skin;

a unit which calculates a change in at least one function associated with the effect of thermal stimulation on a change  
 in light absorption by hemoglobin as a result of the effect of temperature on glucose metabolism;

a unit which calculates a change in at least one function associated with the effect of thermal stimulation on a change  
 in light attenuation as a result of a change in light scattering and blood flow;

a unit which derives a calibration relationship between a combination of the calculated functions derived from the  
 localized reflectance signals and a glucose concentration; and

a unit which uses the measurement and the established calibration relationship for predicting a glucose concentration  
 in a subject at a subsequent time, wherein the calculation units are adapted to calculate a degree of change in light  
 absorption as a function associated with the time dependent effect of the temperature on the localized reflectance  
 values at a plurality of wavelengths and light source (6)-detector (7) distances, wherein the degree of change is  
 calculated for at least one time window, **characterized in that** the degree of change in light absorption is averaged  
 over at least two adjacent time windows using a moving average calculation.

## Patentansprüche

1. Verfahren zur nicht-invasiven Messung von Glukose mittels der Intensität von reflektiertem Licht, die sich gemäß  
 der Lichtstreuung und Lichtabsorption durch eine Hämoglobinvariante als biologischer Index mit einer intensiven  
 Farbe ändert, umfassend die Schritte:

Inkontaktbringen einer optischen Sonde für eine lokalisierte Reflexion, deren Temperatur zu einer Temperatur  
 moduliert worden ist, die sich von der normalen Hauttemperatur unterscheidet, mit Haut zum Induzieren einer  
 Veränderung des Glukosestoffwechsels in einem Nährstoffkapillargefäß in der Haut und Verändern der Kon-  
 zentration einer-Hämoglobin-variante als Veränderung des Glukosestoffwechsels,  
 Auswählen eines Zeitfensters zum Sammeln von Daten, in dem ein Gewebe-Sonde-Anpassungseffekt auf das

resultierende Signal klein ist,

Messen einer Veränderung der lokalisierten reflektierten Lichtsignale bezüglich verschiedener Lichtquelle (6)-Detektor (7)-Abstände, verschiedener Wellenlängen und verschiedener Kontaktzeiten während einer festgelegten Zeit ausgehend von dem Kontakt der Sonde mit der Haut,

Berechnen einer Veränderung mindestens einer Funktion, die mit dem Effekt der thermischen Anregung auf eine Veränderung der Lichtabsorption durch Hämoglobin als Ergebnis des Effekts der Temperatur auf den Glukosestoffwechsel zusammenhängt,

Berechnen einer Veränderung mindestens einer Funktion, die mit dem Effekt der thermischen Anregung auf eine Veränderung der Lichtabschwächung als Ergebnis einer Veränderung der Lichtstreuung und des Blutflusses zusammenhängt,

Ableiten einer Kalibrierungsbeziehung zwischen einer Kombination der berechneten Funktionen, die von den lokalisierten Reflexionssignalen und einer Glukosekonzentration abgeleitet sind, und

Verwenden der Messung und der erstellten Kalibrierungsbeziehung zum Vorhersagen einer Glukosekonzentration in einem Lebewesen zu einem späteren Zeitpunkt,

wobei der Berechnungsschritt den Schritt des Berechnens eines Grads der Veränderung der Lichtabsorption als eine Funktion, die mit dem zeitabhängigen Effekt der Temperatur auf die lokalisierten Reflexionswerte zusammenhängt, bei einer Mehrzahl von Wellenlängen und Lichtquelle (6)-Detektor (7)-Abständen umfasst, wobei der Grad der Veränderung für mindestens ein Zeitfenster berechnet wird, **dadurch gekennzeichnet, dass** der Grad der Veränderung der Lichtabsorption über mindestens zwei benachbarte Zeitfenster unter Verwendung einer Berechnung des gleitenden Durchschnitts gemittelt wird.

2. Verfahren nach Anspruch 1, bei dem der maximale Lichtquelle (6)-Detektor (7)-Abstand in der Sonde für eine lokalisierte Reflexion 2 mm oder weniger beträgt.

3. Vorrichtung zur nicht-invasiven Messung von Glukose, die eine Intensität von reflektiertem Licht nutzt, die sich gemäß der Lichtstreuung und Lichtabsorption durch eine Hämoglobinvariante als biologischer Index mit einer intensiven Farbe ändert, umfassend

eine Einheit (2), welche die Temperatur einer optischen Sonde für eine lokalisierte Reflexion, die mit Haut zum Induzieren einer Veränderung des Glukosestoffwechsels in einem Nährstoffkapillargefäß in der Haut und Verändern der Konzentration einer Hämoglobinvariante als Veränderung des Glukosestoffwechsels in Kontakt gebracht worden ist, zu einer Temperatur moduliert, die sich von der normaten Hauttemperatur wesentlich unterscheidet,

eine Einheit, die ein Zeitfenster zum Sammeln von Daten auswählt, in dem ein Gewebe-Sonde-Anpassungseffekt auf das resultierende Signal klein ist,

eine Einheit, die eine Veränderung der lokalisierten reflektierten Lichtsignale bezüglich verschiedener Lichtquelle (6)-Detektor (7)-Abstände, verschiedener Wellenlängen und verschiedener Kontaktzeiten während einer festgelegten Zeit ausgehend von dem Kontakt der Sonde mit der Haut misst,

eine Einheit, die eine Veränderung mindestens einer Funktion berechnet, die mit dem Effekt der thermischen Anregung auf eine Veränderung der Lichtabsorption durch Hämoglobin als Ergebnis des Effekts der Temperatur auf den Glukosestoffwechsel zusammenhängt,

eine Einheit, die eine Veränderung mindestens einer Funktion berechnet, die mit dem Effekt der thermischen Anregung auf eine Veränderung der Lichtabschwächung als Ergebnis einer Veränderung der Lichtstreuung und des Blutflusses zusammenhängt,

eine Einheit, die eine Kalibrierungsbeziehung zwischen einer Kombination der berechneten Funktionen ableitet, die von den lokalisierten Reflexionssignalen und einer Glukosekonzentration abgeleitet sind, und

eine Einheit, welche die Messung und die erstellte Kalibrierungsbeziehung zum Vorhersagen einer Glukosekonzentration in einem Lebewesen zu einem späteren Zeitpunkt nutzt, wobei die Berechnungseinheiten zum Berechnen eines Grads der Veränderung der Lichtabsorption als eine Funktion, die mit dem zeitabhängigen Effekt der Temperatur auf die lokalisierten Reflexionswerte zusammenhängt, bei einer Mehrzahl von Wellenlängen und Lichtquelle (6)-Detektor (7)-Abständen angepasst sind, wobei der Grad der Veränderung für mindestens ein Zeitfenster berechnet wird, **dadurch gekennzeichnet, dass** der Grad der Veränderung der Lichtabsorption über mindestens zwei benachbarte Zeitfenster unter Verwendung einer Berechnung des gleitenden Durchschnitts gemittelt wird.

## Revendications

1. Procédé pour la mesure non-invasive du glucose utilisant une intensité lumineuse réfléchie changeant en fonction de la dispersion de la lumière et de l'absorption de la lumière par une variante de l'hémoglobine comme indicateur biologique avec une couleur forte, comprenant les étapes suivantes de :

amener une sonde de réflectance optique localisée dont la température a été modulée à une température substantiellement différente de la température normale de la peau en contact avec la peau pour induire un changement dans le métabolisme du glucose dans un capillaire nutritif de la peau et changer la concentration d'une variante de l'hémoglobine comme le changement du métabolisme du glucose ;  
 5 choisir une fenêtre de temps pour collecter les données, dans laquelle un effet d'adaptation tissu-échantillon sur le signal résultant est faible ;  
 mesurer un changement des signaux de lumière réfléchiés localisés par rapport aux diverses distances source lumineuse (6)-détecteur (7), aux diverses longueurs d'onde et aux divers temps de contact pendant un temps spécifié à partir du contact de la sonde avec la peau ;  
 10 calculer un changement d'au moins une fonction associée à l'effet de stimulation thermique sur un changement d'absorption de lumière par l'hémoglobine comme résultat de l'effet de la température sur le métabolisme du glucose ;  
 calculer un changement d'au moins une fonction associée à l'effet de stimulation thermique sur un changement d'atténuation de la lumière comme résultat d'un changement de dispersion de la lumière et de débit sanguin ;  
 15 dériver une relation de calibration entre une combinaison des fonctions calculées dérivées des signaux de réflectance localisés et d'une concentration de glucose ; et  
 utiliser la mesure et la relation de calibration établie pour prévoir une concentration de glucose dans un sujet à un temps ultérieur,  
 dans lequel l'étape de calcul comprend l'étape de calcul du degré de changement d'absorption de lumière  
 20 comme une fonction associée à l'effet assujéti au temps de la température sur les valeurs localisées de réflectance à une pluralité de longueurs d'ondes et distances source lumineuse (6)-détecteur (7), dans lesquelles le degré de changement est calculé pour au moins une fenêtre de temps, **caractérisé en ce que** le degré de changement d'absorption de lumière est une moyenne sur au moins deux fenêtres de temps adjacentes utilisant un calcul de moyenne mobile.

- 25
2. Procédé selon la revendication 1, dans lequel la distance source lumineuse (6)-détecteur (7) maximale dans la sonde de réflectance localisée est de 2 mm ou moins.
  3. Dispositif pour la mesure non-invasive du glucose, utilisant une intensité lumineuse réfléchiée changeant en fonction de la dispersion de la lumière et de l'absorption de la lumière par une variante de l'hémoglobine comme indicateur biologique avec une couleur forte, comprenant :  
 30

une unité (2) modulant la température d'une sonde de réflectance optique localisée qui a été mise en contact avec la peau pour induire un changement du métabolisme du glucose dans un capillaire nutritif de la peau et changer la concentration d'une variante de l'hémoglobine comme le changement du métabolisme du glucose, à une température substantiellement différente de la température normale de la peau ;  
 35 une unité choisissant une fenêtre de temps pour collecter les données, dans laquelle un effet d'adaptation tissu-échantillon sur les signaux résultants est faible ;  
 une unité mesurant un changement des signaux de lumière réfléchiés localisés par rapport aux diverses distances source lumineuse (6)-détecteur (7), aux diverses longueurs d'onde et aux divers temps de contact pendant un temps spécifié à partir du contact de la sonde avec la peau ;  
 40 une unité calculant un changement d'au moins une fonction associée à l'effet de stimulation thermique sur un changement d'absorption de lumière par l'hémoglobine comme résultat de l'effet de la température sur le métabolisme du glucose ;  
 45 une unité calculant un changement d'au moins une fonction associée à l'effet de stimulation thermique sur un changement d'atténuation de la lumière comme résultat d'un changement de dispersion de la lumière et de débit sanguin ;  
 une unité dérivant une relation de calibration entre une combinaison des fonctions calculées dérivées des signaux de réflectance localisés et d'une concentration de glucose ; et  
 50 une unité qui utilise la mesure et la relation de calibration établie pour prévoir une concentration de glucose dans un sujet à un temps ultérieur, dans lequel les unités de calcul sont adaptées à calculer un degré de changement d'absorption de lumière comme une fonction associée à l'effet assujéti au temps de la température sur les valeurs localisées de réflectance à une pluralité de longueurs d'ondes et distances source lumineuse (6)-détecteur (7), dans lesquelles le degré de changement est calculé pour au moins une fenêtre de temps, **caractérisé en ce que** le degré de changement d'absorption de lumière est une moyenne sur au moins deux  
 55 fenêtres de temps adjacentes utilisant un calcul de moyenne mobile.

FIG. 1

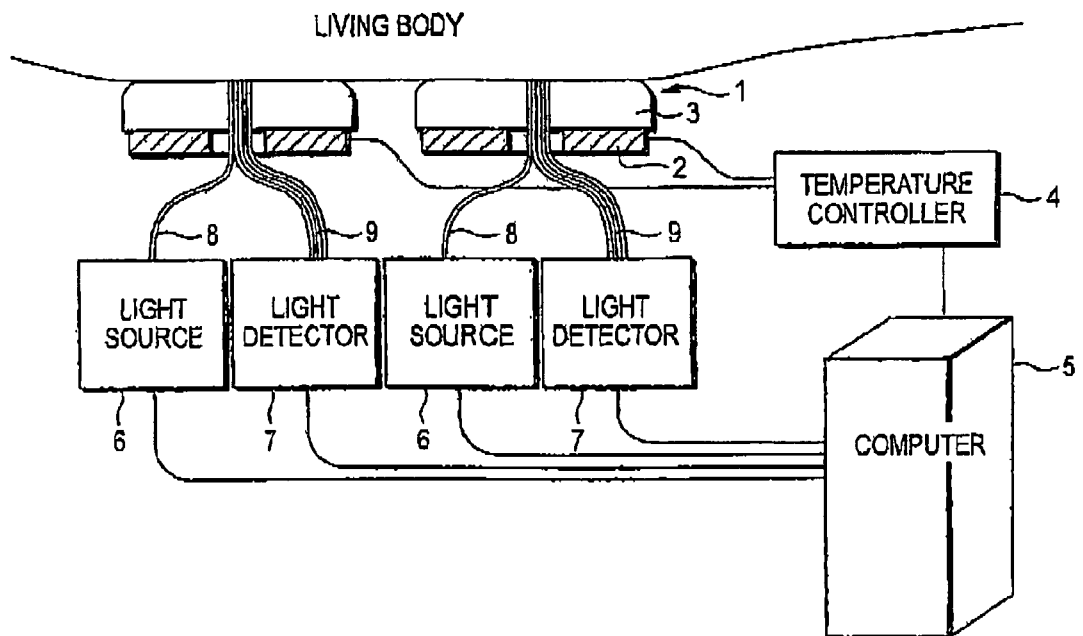


FIG. 2

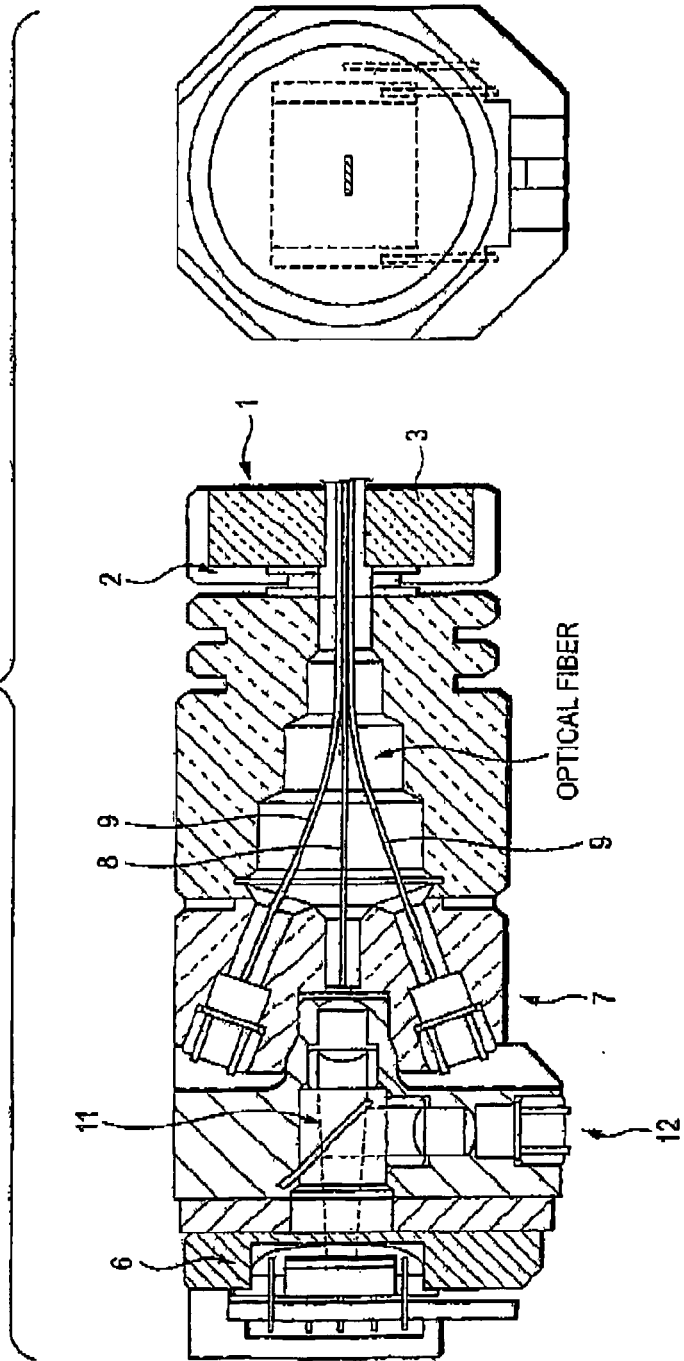


FIG. 3

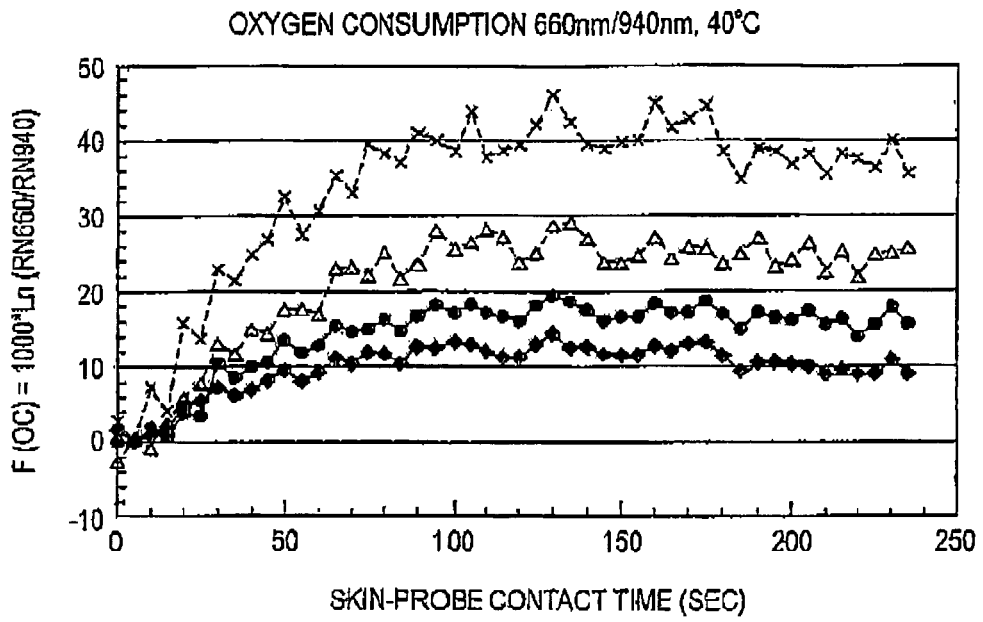


FIG. 4

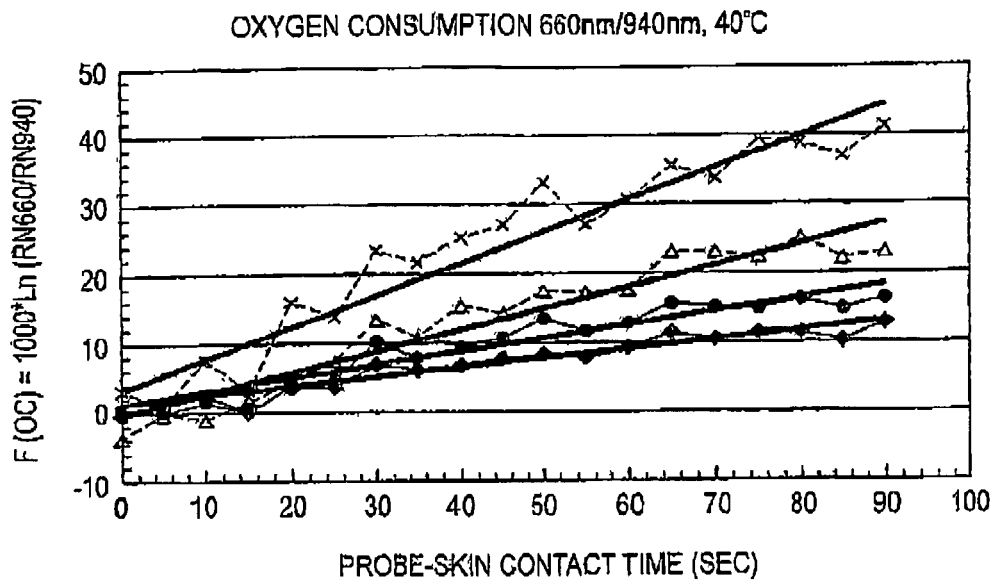


FIG. 5

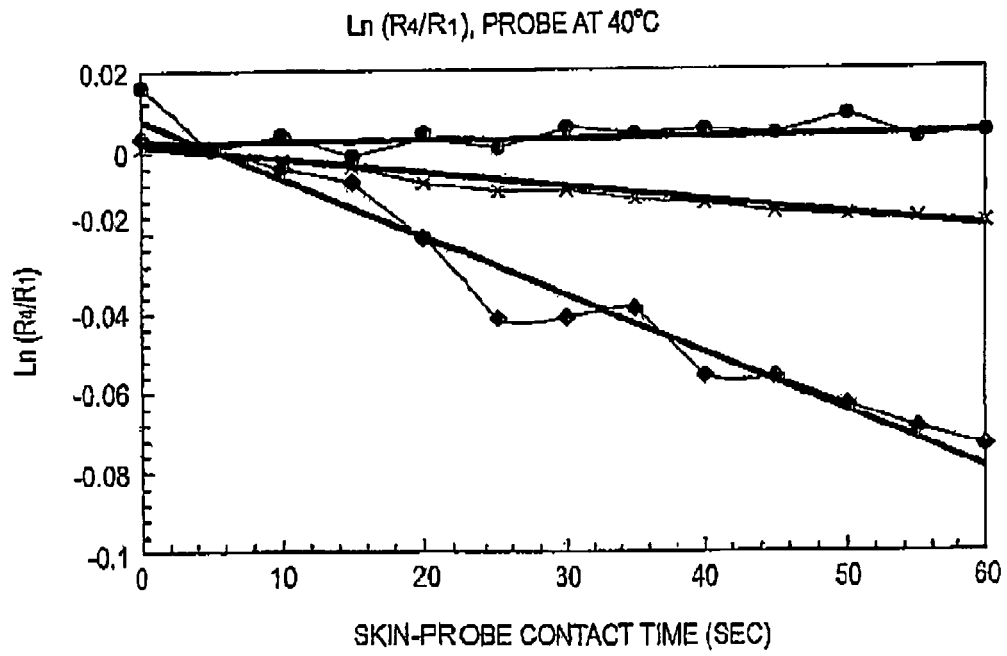


FIG. 6

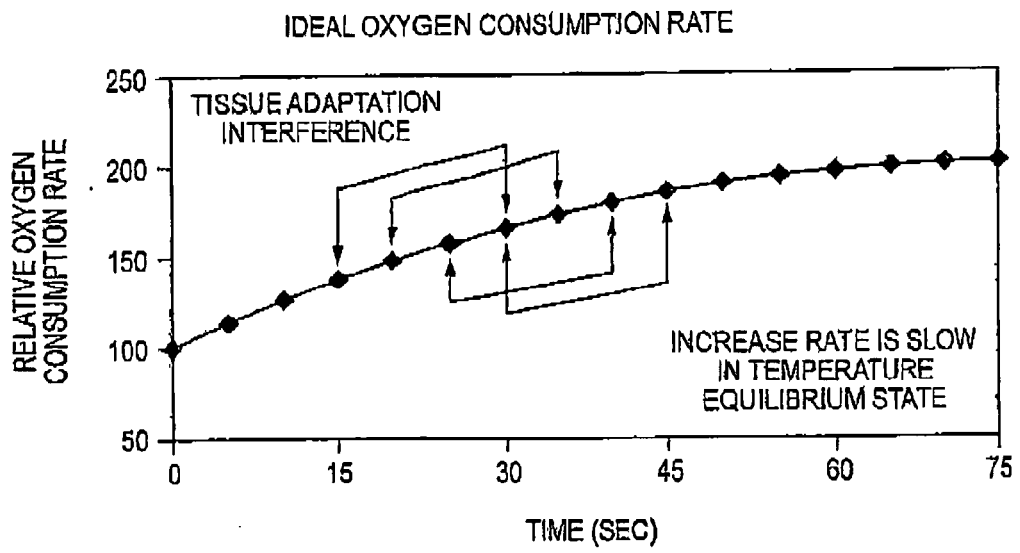


FIG. 7A

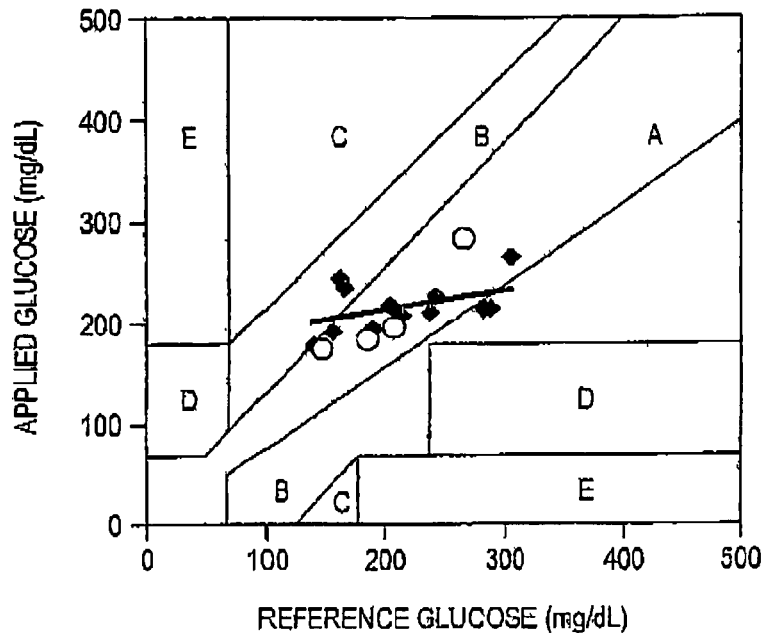


FIG. 7B

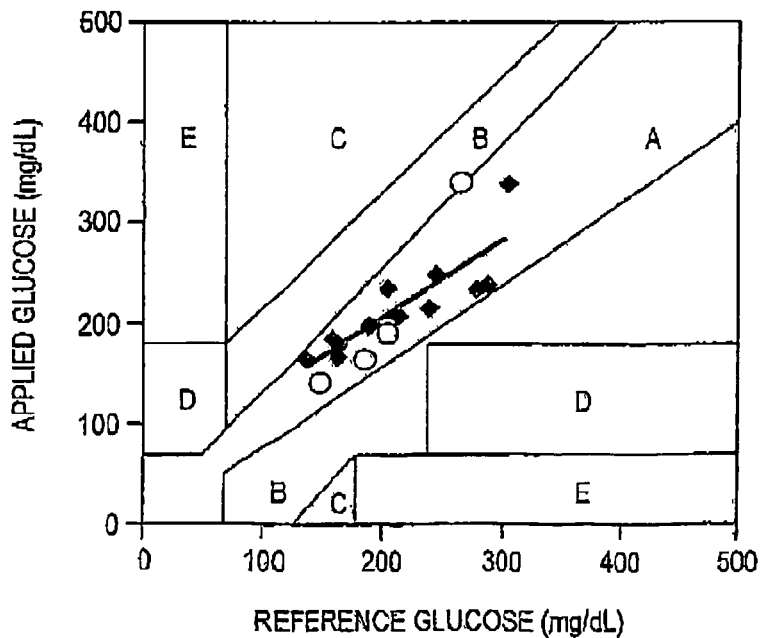


FIG. 7C

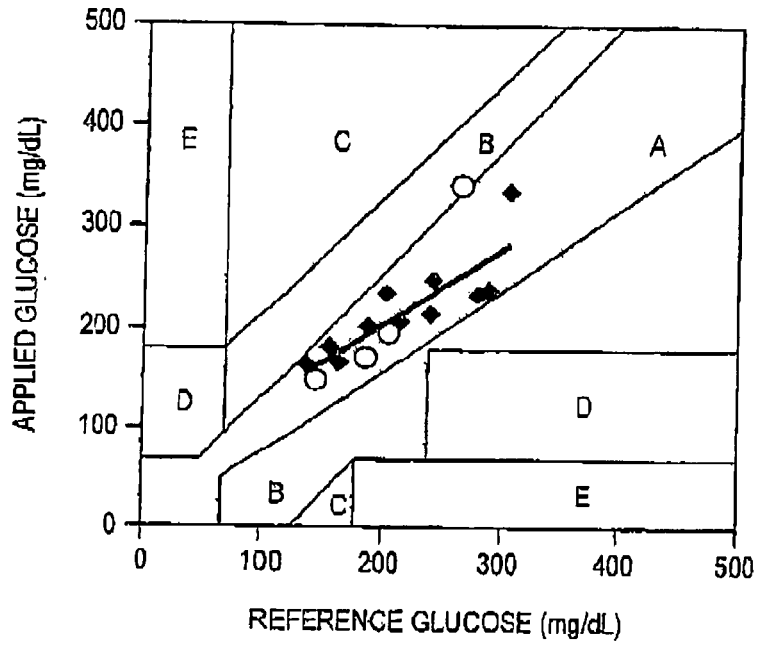
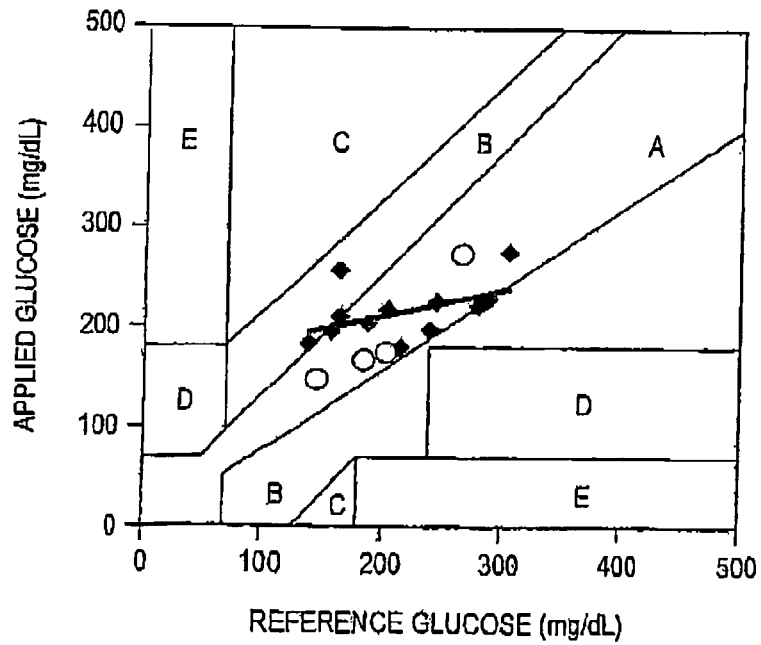


FIG. 7D



## REFERENCES CITED IN THE DESCRIPTION

This list of references cited by the applicant is for the reader's convenience only. It does not form part of the European patent document. Even though great care has been taken in compiling the references, errors or omissions cannot be excluded and the EPO disclaims all liability in this regard.

## Patent documents cited in the description

- US 5077476 A [0029]
- US 5068536 A [0029]
- US 5576544 A [0029]
- US 5703364 A [0029]
- US 5028787 A [0029]
- US 5086229 A [0029]
- US 5324979 A [0029]
- US 5237178 A [0029]
- US 5360004 A [0029]
- US 5460177 A [0029]
- US 5379764 A [0029]
- US 5747806 A [0029]
- US 5945676 A [0029]
- US 6280381 B [0029]
- US 5957841 A [0029]
- US 6016435 A [0029]
- US 5636633 A [0029]
- US 5655530 A [0029]
- US 6230034 B [0029]
- US 5551422 A [0029] [0040]
- US 5492118 A [0029] [0040]
- US 6049081 A [0029]
- US 6556850 B [0029]
- US 5795305 A [0029] [0084]
- US 5924996 A [0029] [0084] [0085]
- US 20050124868 A [0029] [0084]
- EP 1537822 A [0029] [0084]
- US 5940182 A [0029]
- US 3628525 A [0029]
- US 4259963 A [0029]
- US 4432365 A [0029]
- US 4890619 A [0029]
- US 4926867 A [0029]
- US 5131391 A [0029]
- US 5978691 A [0029] [0084] [0085]
- WO 02082989 A1 [0030]
- US 6662030 B, Khalil [0034] [0050]
- US 5785305 A [0085]
- US 6654620 B [0088]

## Non-patent literature cited in the description

- **AMEROV et al.** Molar absorptivities of glucose and other biological molecules in aqueous solutions over the first overtone and combination regions of the near-infrared spectrum. *Applied Spectroscopy*, 2004, vol. 58, 1195-1204 [0029]
- **ROBINSON et al.** Noninvasive glucose monitoring in diabetic patients: a preliminary evaluation. *Clinical Chemistry*, September 1992, vol. 38 (9), 1618-22 [0029]
- **MAIER et al.** Non-invasive glucose determination by measuring variations of the reduced scattering coefficient of tissues in the near-infrared. *Optics Letter*, 1994, vol. 19, 2062-64 [0029]
- **KOHL et al.** Influence of glucose concentration on light scattering in tissue stimulating phantoms. *Optics Letters*, 1994, vol. 19, 2170-72 [0029]
- **KOHL et al.** The influence of glucose concentration upon the transport of light in tissue-stimulating phantoms. *Physics Medicine Biology*, 1995, vol. 40, 1267-87 [0029]
- **HEINMANN et al.** *Diabetes Technology Therapeutics*, 2000, vol. 2, 211-220 [0029]
- **LAUFER et al.** Effect of temperature on the optical properties of ex vivo human dermis and subdermis. *Phys. Med. Biol.*, 1998, vol. 43, 2479-2489 [0029]
- **BRUULSEMA et al.** Optical Properties of Phantoms and Tissue Measured in vivo from 0.9-1.3  $\mu\text{m}$  using Spatially Resolved Diffuse Reflectance. *SPIE Proceedings*, 1997, vol. 2979, 325-334 [0029]
- **KHALIL et al.** Temperature modulation of the visible and near infrared absorption and scattering coefficients of intact human skin. *J Biomedical Optics*, 2003, vol. 8, 191-205 [0029]
- **YEH et al.** Near Infrared Thermo-Optical Response of The Localized Reflectance of Intact Diabetic and Non-Diabetic Human Skin. *J Biomedical Optics*, 2003, vol. 8, 534-544 [0029]
- **YEH et al.** Tracking Blood Glucose Changes in Cutaneous Tissue by Temperature-Modulated Localized Reflectance Measurements. *Clinical Chemistry*, 2003, vol. 49, 924-934 [0029]
- **KHALIL et al.** Response of near IR localized reflectance signals of intact diabetic human skin to thermal stimuli. *SPIE Proceedings*, 2003, vol. 5086, 142-148 [0029]
- **CHO et al.** Noninvasive measurement of glucose by metabolic heat conformation method. *Clinical Chemistry*, 2004, vol. 50, 1984-1988 [0029]

## EP 2 243 425 B1

- **KO et al.** Body metabolism provides a foundation for noninvasive blood glucose monitoring. *Diabetes Care*, 2004, vol. 27, 1211-2 [0029]
- **MALCHOFF et al.** A novel noninvasive blood glucose monitor. *Diabetes Care*, 2002, vol. 25, 2268-75 [0029]
- **HEINEMANN et al.** *Diabetes Technology Therapeutics*, 2000, vol. 2, 211-220 [0029]
- **KHALIL et al.** *J. Biomed. Opt.*, 2003, vol. 8, 191-205 [0034]
- **YEH et al.** *J. Biomed. Opt.*, 2003, vol. 8, 534-44 [0034]
- **YEH et al.** *Clin. Chem.*, 2003, vol. 49, 924-34 [0034]
- *Diabetes Technology and Therapeutics*, 2000, vol. 2, 211-220 [0040]
- *J. Biomedical Optics.*, 2003, vol. 8, 191-205 [0091]

专利名称(译)	用于无创测量葡萄糖的方法和用于无创测量葡萄糖的装置		
公开(公告)号	<a href="#">EP2243425B1</a>	公开(公告)日	2014-08-13
申请号	EP2010170622	申请日	2006-11-30
[标]申请(专利权)人(译)	东芝医疗系统株式会社		
申请(专利权)人(译)	东芝医疗系统公司		
当前申请(专利权)人(译)	东芝医疗系统公司		
[标]发明人	KANAYAMA SHOICHI KHALIL OMAR S JENG TZYU WEN YEH SHU JEN		
发明人	KANAYAMA, SHOICHI KHALIL, OMAR, S. JENG, TZYU-WEN YEH, SHU-JEN		
IPC分类号	A61B5/1455 A61B5/00		
CPC分类号	A61B5/1455 A61B5/0053 A61B5/14532 A61B5/1491 A61B5/1495 A61B5/6824 A61B5/6843		
代理机构(译)	KRAMER - HARSH - 施密特陈		
优先权	2006129490 2006-05-08 JP 2005347194 2005-11-30 JP		
其他公开文献	EP2243425A3 EP2243425A2		
外部链接	<a href="#">Espacenet</a>		

摘要(译)

一种用于非侵入性地测量受试者组织中的葡萄糖的方法，包括使具有类似于测量探针的形状的适配装置与受试者的皮肤部分接触以拉伸受试者的皮肤部分的步骤在非侵入性测量期间，在高于测量探针施加的每单位面积压力的压力下，保持接触一段预定时间，然后缓解接触，使测量探针与拉伸的皮肤部分接触用于非侵入性测量的受试者，收集从受试者发射的信号，并基于收集的信号估计葡萄糖浓度。

$$d[G]/dt = -k_1[G]_{ABC} \quad (1)$$